AD-A045 317 VIRGINIA POLYTECHNIC INST AND STATE UNIV BLACKSBURG --ETC F/G 20/4
TRANSONIC SHOCK-TURBULENT BOUNDARY LAYER INTERACTION WITH SUCTI--ETC(U)
SEP 77 G R INGER, S ZEE N00014-75-C-0456
UNCLASSIFIED VPI-AERO-073 NL

1 OF 1
ADA
045317

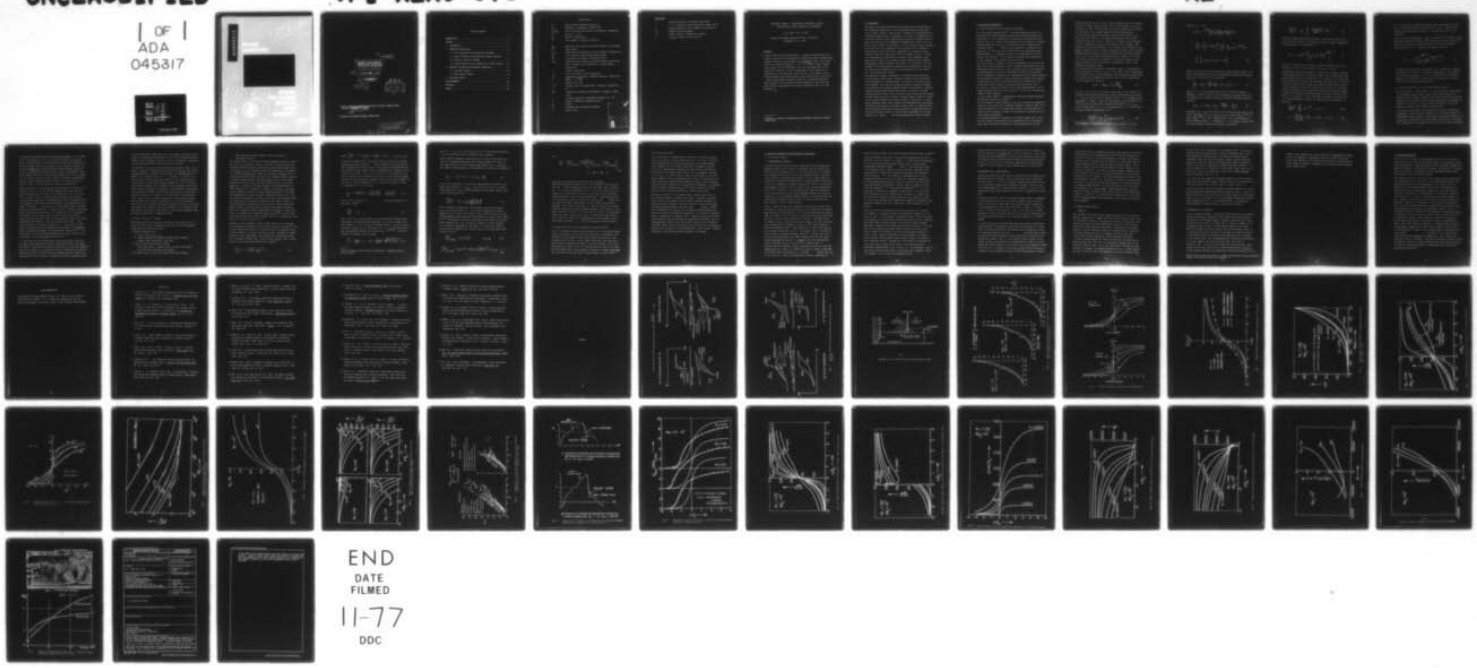

END
DATE
FILMED
11-77
DDC

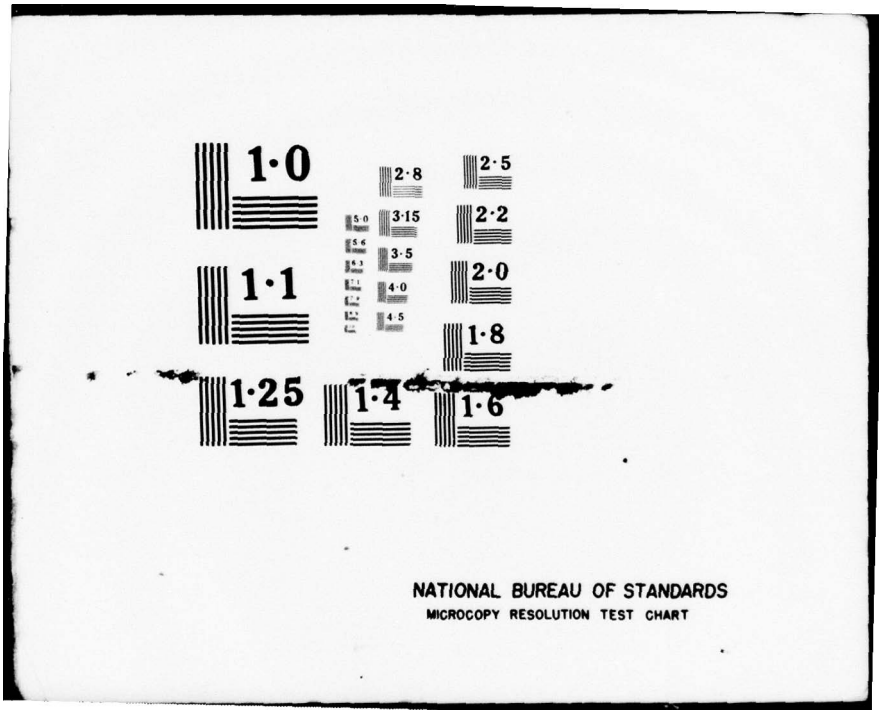
1·0
1·1
1·25
1·4
1·6
1·8
2·0
2·2
2·5
2·8
3·15
3·5
4·0
4·5
5·0
5·6
NATIONAL BUREAU OF STANDARDS
MICROCOPY RESOLUTION TEST CHART

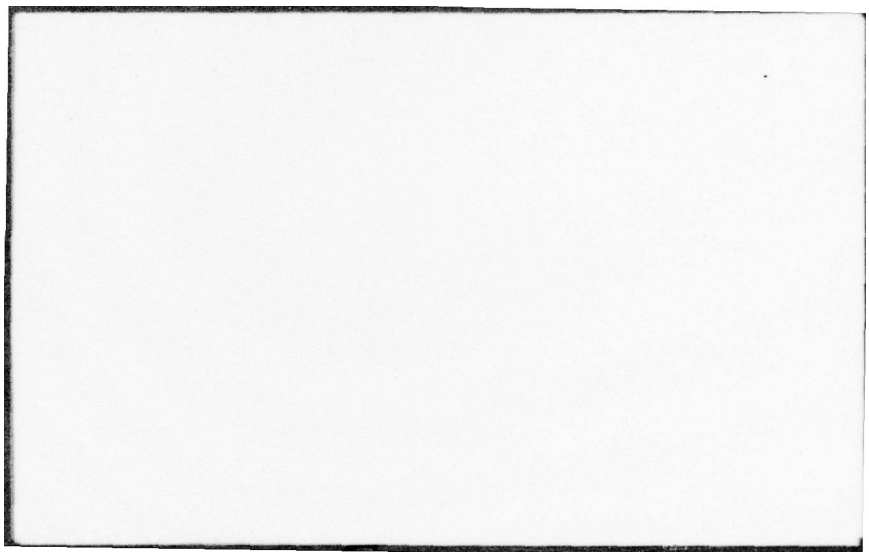

(14) VPI-AERO-073

(6) TRANSONIC SHOCK-TURBULENT BOUNDARY LAYER INTERACTION WITH SUCTION AND BLOWING

(10) G. R. Inger and S. Zee†

(11) Sept[redacted]977

(12) 56 p.

* Based on Research supported by the Office of Naval Research under Contract ONR-N00014-75-C-0456.

(15)

† Professor and Graduate Student, Respectively.

406 922

Table of Contents

Nomenclature

B	mass transfer parameter $\dot{m}_w/\rho_{e_t} U_{e_t}$
$B_{1,2}$	constants in asymptotic solution, Eq. 7
C_{fo}, C_f'	basic flow skin friction and its disturbance, respectively
h_i	$p_i' / p_{oi} (i = 1, 2, 3)$
H_i	Fourier transform of h_i
K	Wave number in Fourier transform
$\dot{m}_w$	mass flow rate across wall surface (positive for blowing)
M	Mach number
p_o, p'	undisturbed and disturbance static pressures, respectively
ΔP	static pressure jump across incident shock
Q	unit solution of pressure disturbance Eq. (3)
$Re_{\delta,L}$	Reynolds number based on conditions ahead of shock and either boundary layer thickness or running length L, respectively
T	absolute temperature
u, v	x and y direction velocity components
x, y	streamwise and normal coordinate distances, respectively
β	$\sqrt{M_1^2-1}$ or $\sqrt{1-M_2^2}$
γ	specific heat ratio
δ, δ^*	boundary layer and displacement thickness, respectively
η	y/δ
μ, ν	coefficients of dynamic and kinematic viscosity, respectively
ω	viscosity temperature dependence exponent ($\mu \sim T^{\omega}$)
π	Fourier transform of pressure (Eq. 3)
ρ	density
θ^*	boundary layer momentum thickness
τ	shear stress

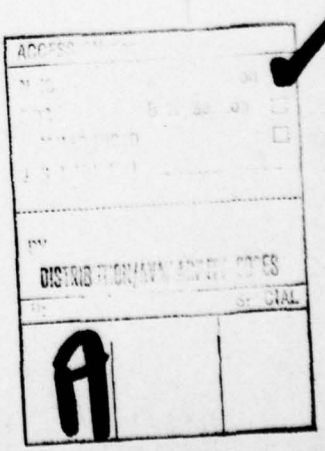

Subscripts

e	Inviscid properties at boundary layer edge
i	i = 1, 2, 3 denotes various disturbance regions (Fig. 1)
0	denotes undisturbed (not stagnation) flow property
LS	Lighthill friction sublayer
ref	Eckert reference temperature condition
w	property evaluated at wall surface

TRANSONIC SHOCK - TURBULENT BOUNDARY LAYER INTERACTION WITH SUCTION AND BLOWING

G. R. Inger and S. Zee*

Virginia Polytechnic Institute and State University,
Blacksburg, Va., USA

Abstract

A basic theory of weak normal shock - turbulent boundary layer interactions is given for two-dimensional non-separating flows including mass transfer across the wall throughout the interaction region. Even small amounts of suction ($-m_w/\rho_e U_e \sim 1$ to 5×10^{-4}) are found to significantly reduce both the streamwise scale and thickening effect of the interaction and delay the onset of separation. This is shown to be a consequence of the large mass transfer effect on the shape of the incoming boundary layer Mach number profile away from the wall. Parametric study results showing the influence of Reynolds and shock Mach number as well as mass transfer parameter on the interaction, plus favorable comparisons with various experimental data, are also presented.

---

* Professor of Aerospace Engineering and Graduate Research Assistant, respectively

1. Introduction

The study of transonic shock-turbulent boundary layer interactions is of well-established importance in the aerodynamic design of high speed aircraft wings, transonic wind tunnels, cascades in turbomachinery and airbreathing engine inlets. Consequently, the control and suppression of interaction effects in these applications by suction or blowing is also of great interest since the technology of boundary layer control (BLC) by surface mass transfer has advanced to a very practical status. Although there have been some experimental investigations of BLC applied to shock-boundary layer interaction suppression in supersonic inlets [1] transonic wind tunnel side walls [2] and on transonic airfoils [3,4] which have established the desirability of the idea, little systematic basic study has been done in the transonic regime, especially with regard to establishing a sound theoretical framework for the problem. It is the purpose of the present paper to develope such a fundamental theory for the restricted but important case of non-separating flow with normal wall (unvectored) mass transfer.

Our approach is based on extending a recently-developed analytical theory of weak normal shock - turbulent boundary layer interactions[5] on the premise that, notwithstanding the existance of powerful numerical methods, there will be a continuing need for analytical methods which delineate the essential physical features and parametric trends of transonic shock-boundary layer interactions. In Section 2 the basic formulation and features of the theoretical model including surface mass transfer effects are given. Section 3 presents typical numerical results for zero mass transfer that include a number of heretofore - unpublished Reynolds number effect results and comparisons with experiment, followed by illustrations of the mass transfer effect on important interaction properties with some favorable qualitative comparisons with the little data available. Section 4 concludes with a discussion of the limitations of the theory and recommendations for further studies.

2. Theoretical Formulation

2.1 Basic Features of the Interaction Flow Model

It is well-known experimentally [6,7] that when separation occurs, the disturbance flow pattern associated with normal shock-boundary layer interaction is a very complicated one involving a bifurcated shock pattern (see Fig. 1a), whereas the unseparated case pertaining to turbulent boundary layers up to $M_1 \lesssim 1.3$ has instead a much simpler type of interaction pattern which is more amenable to analytical treatment (Fig. 1b). With the use of some judicious yet physically-sound simplifications, it is possible to construct an approximate analytical theory of the problem. For the sake of orientation and completeness, a brief summary of this theory will now be given.

The flow is taken to consist of a known unseparated turbulent boundary layer profile $M_o(y)$ subjected to small transonic disturbances due to an impinging weak normal shock. Our theoretical model of this interaction is a simplification of the small disturbance flow structure emerging from an asymptotic analysis of the compressible Navier-Stokes equations at high Reynolds numbers[8], giving a linearized boundary value problem surrounding the nonlinear shock discontinuity and underlaid by a thin viscous disturbance sublayer as schematically illustrated in Fig. 2.

To achieve an analytical solution in the leading approximation, the following assumptions are introduced (see Ref. 5,8 for more detailed discussion of their validity).

(a) The incident shock is a discontinuity across which Rankine-Hugoniot shock jump relations are satisfied.

(b) The nonlinear transonic terms in the outer inviscid flow regions are neglected, since most of the significant nonlinear transonic effect is already accounted for in the shock jump relations. We thus deal with a linearized (but rotational) boundary value problem surrounding the nonlinear shock discontinuity.

(c) Following Lighthill's treatment of the oblique shock case[9], we impose the incident normal shock jump conditions only at the boundary layer edge and neglect the details of the shock pentration into the

underlying region; since the correct shock pressure jump at the edge is accounted for while below the sonic level in the boundary layer no discontinuity can exist, the shock decay across the supersonic non-uniform flow region is in fact roughly simulated by this approximation.

(d) The viscous disturbance sublayer is assumed thin enough to lie within the linear portion of the undisturbed boundary layer profile [9]. Provided M_1 is not so close to unity that the incident shock thickness becomes a significant fraction of the boundary layer thickness, this approximate flow model contains all the essential global features of the mixed transonic character of the non-separating normal shock-turbulent boundary layer interaction problem including lateral pressure gradient effects over a wide range of Reynolds numbers. Moreover, the linearized theory involved is now amenable to analytical treatment by obtaining solutions in each of the three regions shown in Fig. 2 and appropriate matching of them.

The linearized small disturbance supersonic region 1 is governed by the wave equation. Thus if $\eta = \eta_1(x)$ is the small vertical displacement of the interface due to shock interaction and incoming wave disturbances are ruled out, the pressure perturbation about the local undisturbed value far upstream is given by

$$p_1'(x) \simeq (\rho_{o1} U_{o1}^2/\beta_1)\left(\frac{\partial \tilde{\eta}_1}{\partial x}\right)_{y=0} \qquad (1)$$

where $\tilde{\eta}_1 = \eta_1(x - \beta_1 y)$. The subsonic disturbance flow in quadrant 3 is caused by the interaction-generated interface displacement $\eta_3(x)$ along $y = \delta$ plus the post-shock perturbations along $x = 0^+$ resulting from the impingement of region 1 Mach wave disturbances on the shock*. The solution for the local post-shock pressure perturbation $p_3' = p - p_{o3}$ which vanishes both at $x = 0$, $y \to \infty$ and $x \to \infty$, $y = 0$ can be found by Fourier Sine transformation to be [5]

$$\frac{p_3'(x,y)}{p_{o3}} = \frac{2}{\pi}\int_0^\infty p_3(\hat{y},k)\sin kx\, dk \qquad (2A)$$

*For example, the shock jump relations give $p'_3(0,y) \simeq -p'_1(0,y)$

where $\hat{y} \equiv y - \delta$ and

$$p_3(\hat{y},k) = e^{-k\beta_3\hat{y}} \int_o^\infty \left[\frac{\partial}{\partial y}\left(\frac{p_3'}{p_{o3}}\right)\right]_{\hat{y}=o} \left(\frac{\sin k\,\bar{x}}{k\,\beta_3}\right) d\bar{x}$$

$$+ \frac{M_3^2}{M_1^2}\,\beta_3 \left[\cosh k\beta_3\hat{y} \int_o^\infty \frac{M_3^2}{M_1^3}\,\frac{p_1'}{p_{o1}}(-\beta_1\eta)\, e^{-k\beta_3\eta}\, d\eta \right.$$

$$\left. + \int_o^\infty \frac{p_1'}{p_{o1}}(-\beta_1\eta) \sinh k\beta_3(\eta - \hat{y})\, d\eta \right] \qquad (2B)$$

Within the rotational inviscid disturbance boundary layer region 2, the Fourier transform $\pi(k,y)$ of the non-dimensional disturbance pressure $p_2'/p_{o1}(x,y)$ is governed by the equation[9]

$$\frac{d^2\pi}{d\eta^2} - \frac{2}{M_o}\left(\frac{dM_o}{d\eta}\right)\frac{d\pi}{d\eta} - k^2(1 - M_o^2)\,\pi = 0 \qquad (3)$$

where $y/\delta \equiv \eta$. The solution obeys the inner boundary condition $(d\pi/d\eta)_w = 0$ along the effective wall position $\eta_w = \eta_{LS}$ (see below) and the following outer condition obtained by pressure matching along the interface:

$$\pi(k,\eta = 1) = H_2(k) = H_1(k) + \frac{\Delta p/p_{o1}}{ik} + \frac{p_{o3}}{p_{o1}} H_3 \qquad (4)$$

where $\Delta p \equiv p_{o3} - p_{o1}$ is the basic normal shock jump and $H_2(k)$ is the Fourier transform of $h_2(x) \equiv p_2'(x,1)/p_{o1}$ while $H_1(k) = \int_{-\infty}^{o} h_1 e^{-ikx}\, dx$, $H_3(k) = \int_o^\infty h_3 e^{-ikx}\, dx$. Then introducing the "unit" solution $Q(k,\eta)$ of Eq. (3) satisfying $Q(k,0) = 1$, $dQ/d\eta\,(k,0) = 0$, the general solution with the stated boundary conditions in physical variables is

$$\frac{p_2'(x,\eta)}{p_{o1}} = \frac{1}{2\pi} \int_{-\infty}^{\infty} \frac{Q(k,\eta)H_2(k)}{Q(k,1)} e^{ikx}\, dk \qquad (5)$$

Within the viscous disturbance sublayer, a well-known solution[9] for a linear basic flow profile $U_o \simeq (\tau_w/\mu_w)y$ yields the sublayer displacement thickness (effective wall position):

$$\eta_w \cong .776\left(\frac{1}{\kappa_1}\right)^{1/3}\left[\frac{1}{R_{e_\delta}^{\,2}}\ \frac{2}{C_f}\ \left(\frac{T_w}{T_e}\right)^{1+2\omega}\right]^{1/3} \qquad (6)$$

where κ_1 is the large scale upstream influence parameter defined by Lighthill in terms of the properties of the function $\pi(x,y)$.

Applying these regional solutions to the interfacial matching conditions of continuous pressure and streamline slope at the boundary layer edge yields integro-differential equations for the transform of the interaction pressure along the interface both upstream and downstream of the shock; the details including their lengthy but straightforward solution by operational methods are described in Refs. 5, 8. Inversion by the method of residues and use of the convolution theorem then yields the physical pressure perturbation distributions along the interface and also along the wall. In particular, the wall disturbance pressure is found to have the following asymptotic behavior far upstream and downstream, respectively:

$$\frac{p_2'(x,0)}{\Delta p} \simeq \sum_{\eta=1}^{\infty} B_1 e^{\kappa_\eta x}, \qquad x \ll 0 \qquad (7A)$$

$$\simeq 1 + \frac{2p_{o3}/p_{o1}}{(M_1/M_3)^2}\left[\frac{B_2}{x} + 0\,(x^{-3})\right], \qquad x \gg 0 \qquad (7B)$$

Eq. 7A describes an exponential pressure decay with upstream distance with a characteristic upstream distance scale $\sim(\alpha_1)^{-1}$, whereas (7B) predicts far downstream an algebraic (1/x)- type decay of the local disturbance.

Under the present assumptions, Inger's solution [10] for the shear stress perturbation within the viscous disturbance sublayer can be carried over directly to the present problem; in terms of the surface pressure and a function $F(\alpha)$ of the properties of $\pi(K, y)$ as follows:

$$C'_f(x) = - \frac{(T_w/T_e)^{\frac{1+2\omega}{3}} \int_{-\infty}^{\infty} F(K)\, \pi_w e^{ikx}\, dk}{(Re_\delta^2\, C_{fo})^{1/3}} \qquad (8)$$

Although this integral has a branch point at the origin which makes it very difficult to evaluate for the upper complex plane values required for a downstream solution ($x > 0$), the integration can be done[8] by residues for the important region under and upstream of the shock with the result expressed in terms of p_w'.

2.2 Typical Features of the Zero Mass Transfer Solution

The unit solution $\pi = Q(k, \eta)$ of Eq. (3) was obtained by outward numerical integration using a Mach number profile $M_o(y)$ based on the accurate turbulent model of Inger and Williams[11], which was developed especially for this purpose and is in good agreement with transonic experimental data (Fig. 3). It can be further extended to include the presence of surface mass transfer as shown below.

As originally constructed, the foregoing theory was concerned with establishing a sound analytical structure and a reliable numerical implementation without regard to computational optimization. However, by subsequent streamlining it has been possible to reduce the calculation time enormously. For example, the use of only two terms in evaluating

the residue series summations involved yields negligible (.1% or less) error in the pressure for $M_1 \geq 1.05$ while cutting the time by two-thirds. Furthermore, use of an approximate closed form expression for the Mach number profile that provides a direct analytical relation for the profile slope dM_o/dy without numerical differentiation further improves the computational efficiency by an order of magnitude[12]. Such improvements result in an IBM 370-158 running time of 10-15 seconds for one complete interaction case including all pressure distributions, boundary layer thickening and skin friction, which provides an economical research tool for parametric studies and applications.

Typical features of the resulting interaction pressure field solution are illustrated in Fig. 4, where both the boundary layer edge and wall pressure distributions are shown. The streamwise extent of the interaction is seen to contract noticeably with increasing shock strength, accompanied as expected by a strengthening of the local pressure jump at the boundary layer edge; these trends agree with experimental findings[7,13]. Moreover, it is seen that the shock-induced lateral pressure gradients are significant within a region of several boundary layer thicknesses upstream and downstream of the shock foot, the wall pressure being higher then the edge ahead of the shock and lower behind it. Further upstream where the wall and edge pressure equalize they decay exponentially with distance. Along the boundary layer edge, a local pressure jump occurs across the shock at $x = 0$ followed by a small region of subsonic post-shock expansion and subsequent recompression, again in qualitative agreement with experimental observations[7,13]. Far downstream, the wall and edge pressures again equalize and rise monotonically to the final post-shock level like $1/x$.

It is noted that the local shock jump at the boundary layer edge and its rapid lateral smoothing across the underlying subsonic flow region that yields a continuous wall pressure distribution are important physical features that cannot be accounted for without considering the $\partial p/\partial y$ effect. Moreover, inclusion of lateral pressure gradients captures another interesting feature: the existence of a subsonic post-shock expansion region

at the boundary layer edge (here due to the change across the normal shock of the upstream compression waves from the interaction-induced boundary layer thickening, see Fig. 1). This is qualitatively confirmed by both experiments[7] and detailed numerical solutions.[14]

To illustrate the accuracy and limitations of the present theory, Fig. 5 shows a comparison between its wall pressure predictions and a more elaborate numerical solution[14] and the pipe flow experimental data of Gadd[13] for an adiabatic flow at $M = 1.12$ and $Re_L = 9.6 \times 10^6$. It is seen that there is good agreement between the two theories when uncorrected for the post-shock channel blockage effect due to the interaction-induced boundary layer thickening; each possesses virtually the same accuracy compared to experiment, both moderately underestimating the upstream influence and overestimating the rate of post-shock pressure recovery as is typical of all such channel flow experiments . Thus, under exactly the same conditions the present theory predicts the interactive wall pressure with essentially the same accuracy as does a far more elaborate and expensive numerical solution, while also accounting for the subsonic post-shock expansion at the boundary layer edge; hence it provides a sound basis for interpreting experimental data and further extension for unseparated flows.

2.3 Effect of Suction or Blowing

Some preliminary study discloses that surface mass transfer can influence the interaction in numerous ways, which can be conveniently broken down by regions as follows.

1.) Basic Undisturbed Flow
   a. Alter values of τ_{wo}, δ_o
   b. Change damping of turbulence across laminar sublayer
   c. Change profile shape away from wall

2.) Viscous Disturbance Sublayer Solution
   New mass transfer - induced profile curvature and normal velocity terms in disturbance equations

3.) Pressure Field in Inviscid Rotational Disturbance Region

New non-parallel mass-transfer terms in governing disturbance equation

The effects under 1.) are by far the most important and will be dealt with below. As regards the others, they may be neglected under the assumed conditions of small-to-moderate normal mass transfer rates ($B \equiv \dot{m}_w/\rho_{e_1} U_{e_1} \lesssim 10^{-3}$) typical of practical applications, according to the following considerations. Under the continued assumption that the viscous disturbance sublayer lies within the laminar sublayer region of a turbulent boundary layer, the mass transfer effect in the leading approximation does not alter the $U_o(y)$ profile curvature but only its slope (τ_w); moreover, this slope change is well-approximated as a linear function of B. Furthermore, studies of solutions to the hydrodynamic stability equations for large Reynolds numbers[15] have shown that including the V_o term for small to moderate B has only a very weak effect on solutions for "parallel shear flow"-type problems; since our equations are very similar in form we infer that the explicit V_o terms may also be neglected in solving both the viscous disturbance sublayer and the overlying inviscid pressure perturbation equations. Thus, to a consistant order of approximation the form of these equations is not significantly changed by mass transfer but only the input values from the incoming basic boundary layer flow, provided B is well below the so-called "blow-off"value.

Consider now the modeling of mass transfer effects on the incoming flow, assuming for simplicity that any such blowing or suction is on the average uniform and normal to the wall and that its streamwise extent is large compared to the short interaction range, extending far enough upstream to have established a well-defined local equilibrium profile in the incoming boundary layer. Then the mass transfer effect on skin friction can be reliably described by the relation[16]

$$\frac{C_f}{C_{fo}} \simeq 1 - 23 \left(\frac{T_{ref}}{T_e} \frac{1}{2C_{fo}} \right)^{1/2} B \qquad (9)$$

where $\frac{T_{ref}}{T_e} \simeq 1 + 0.038M_e^2 + 0.50(\frac{T_w}{T_e} - 1)$ for $\gamma = 1.4$ and C_{fo} here is the zero-blowing value*. According to Eq. (9), suction for example increases τ_w and this should have an influence on the interaction that is qualitatively similar to that of decreasing the Reynolds number. The associated mass transfer effect on boundary layer thickness can be calculated as follows. Since it is well-known that the momentum thickness to boundary layer thickness ratio and the Crocco energy equation solution are both insensitive to moderate amounts of mass transfer[17], we can use the following approximate zero blowing relationship[11] based on a power-law ($U \sim y^{1/N}$) profile:

$$\frac{\delta}{\theta^*} \simeq \frac{(N+1)(N+2)}{N}\left\{1 + \left[\frac{N(\gamma-1)M_e^2}{2(N+1)(N+2)} + \frac{T_w - T_e}{(N+1)T_e}\right]\right\} \qquad (10)$$

where θ^* is found from the momentum equation including mass transfer[17]:

$$\frac{d\theta^*}{dX} = \frac{C_f}{2} + B \qquad (11)$$

and X here is the running length from some upstream reference point. Then under the aforementioned assumption that B is a constant over some region $X_1 \le X \le X_2$ (and zero outside) with X_1, X_2 far in front of and behind, respectively, the interaction zone $X \simeq L$, and using Eq. (9) plus the approximate power law formula $C_{f_o} \sim X^{-2(N+3)}$ to facilitate analytical integration, Eq. (11) yields

$$\frac{\theta^*}{L} \simeq \frac{(N+3)}{2(N+1)} \cdot C_{fo} + B\left[1 - \frac{23(N+3)}{2(N+2)}\sqrt{\left(\frac{T_{ref}/T_e}{2}\right)C_{fo}}\right] \qquad (12)$$

---

* We have used for this a reference temperature - modified Schultz-Grunow relation

with $N \simeq 7$ to 10. Use of this result in Eq. (10) thus enables estimation of the mass transfer effect on boundary layer thickness.

Aside from the foregoing blowing effect on the profile wall slope (τ_w), there is an additional distortion of its detailed shape away from the wall which derives from the following approximate turbulent boundary layer shear stress distribution recommended by Conrad and Donaldson[18]:

$$\frac{\tau}{\tau_w} \simeq 1 - 3\eta^2 + 2\eta^3 + (1 - \eta^2) \cdot \frac{U}{U_e} \cdot \frac{2B}{C_{fo}} \qquad (13)$$

with $\eta \equiv y/\delta$ and where to a good first approximation for weak to moderate mass transfer $U \simeq (U)_{B=0}$ in the last term. Eq. (13) is used in connection with the basic relation defining turbulent shear stress, which can be written in the form

$$\frac{d(U/U_e)}{d\eta} = \frac{C_f}{2} \, Re_{\infty\,\delta} \left(\frac{T}{T_e} \right) \left(\frac{\tau/\tau_w}{\nu_{eff}/\nu_e} \right) \qquad (14)$$

where it remains to specify the total kinematic viscosity distribution ν_{eff} in the turbulent flow. Now, the available experimental evidence suggests that the form of the turbulent eddy viscosity relation is significantly affected only by relatively large amounts of surface mass transfer[17, 19]; provided we account for the mass transfer effect on the parameters involved (e.g., τ_w) we thus can continue to use the existing $B = 0$ viscosity formulation for the weak - to - moderate blowing or suction cases of interest here. Thus we have the two-layer piece-wise continuous model[18]:

$$\left. \frac{\nu_{eff}}{\nu_e} \right|_{INNER} = (T_w/T_e)^{1+\omega}, \qquad \text{for } \eta \leq \eta_s^* \qquad (15A)$$

$$\left. \frac{\nu_{eff}}{\nu_e} \right|_{OUTER} = (T_w/T_e)^{1+\omega} + .051\Gamma Re_\delta \left[\frac{T_{ref} C_f}{2\, Te} \right]^{1/2} \text{for } \eta > \eta_s^* + .16 \qquad (15B)$$

and

$$\frac{\nu_{eff}}{\nu_e} = \left.\frac{\nu_{eff}}{\nu_e}\right|_{INNER} + \left[\frac{\eta-\eta_s^*}{.16}\right]\left[\left.\frac{\nu_{eff}}{\nu_e}\right|_{OUTER} - \left.\frac{\nu_{eff}}{\nu_e}\right|_{INNER}\right] \tag{15C}$$

$$\text{for} \quad \eta_s^* < \eta < \eta_s^* + .16$$

where Γ is the Klebanoff intermittency factor and η_s^* is found by requiring the integral of Eq. 14 to satisfy the no slip condition U(0) = 0 upon integrating forward from the outer initial condition U(1) = U_e. Thus the substitution of Eqs. (13) and (15) plus the Crocco integral for the temperature profile T(u) into Eq. 14 and subsequent integration yields an accurate yet fundamentally - based determination of the incoming turbulent boundary layer velocity and Mach number profiles including compressibility, heat transfer and moderate amounts of wall suction or injection; the results satisfy all the proper boundary conditions including vanishing gradients at the boundary layer edge, conform to the Law of the Wall near the surface, are continuous across the entire boundary layer with a velocity defect-type behavior in the outer part, and are in good agreement with experiment over a wide range of transonic - to - moderately supersonic Mach numbers.

2.4 Typical Features of the Interaction with Mass Transfer

Fig. 6 illustrates the typical mass transfer effect on the Mach number profile, from which it can be seen that this effect is dominated by the influence of mass transfer on the profile shape away from the wall; including only the effect on shear stress (wall slope) badly underestimates both the magnitude and sign of the profile changes. This can be understood by a study of Eq. (13): inserting typical values in the right hand side shows that a given amount of blowing (for example) <u>increases</u> the local shear stress and hence velocity gradient far more than it

reduces the wall slope.

We now examine the consequences of this on the interaction solution itself. Fig. 7 gives a typical result for a $M_1 = 1.10$, $Re_L = 10^6$ interaction, showing how the various contributions to the suction/blowing effect influence the wall pressure distribution (analogous influences occur on the displacement thickness and skin friction). Whereas the contribution of the mass transfer effect on δ_o is negligable compared to that on τ_w, the effect on profile shape is quite large (in fact completely opposite to and overwhelming the τ_w-effect) as indeed would be expected from the aforementioned influence on $M_o(y)$. This conclusion, which was found to apply over a wide range of conditions, is concordant with the finding of Panaras and Inger[12] that the interaction is quite sensitive to the turbulent boundary layer profile form factor.

Referring hereafter to the complete mass transfer model with all three effects included we observe that suction, because of its predominant effect in decreasing the Mach number gradient and hence enhacing the profile "fullness" away from the wall, reduces the streamwise extent and thickening of the interaction, making it appear more inviscid-like in character with a steeper adverse pressure gradient; thus suction is qualitatively equivalent to an increase in Reynolds number. Blowing has the opposite effect, tending to spread out the interaction pressure field and increase the displacement thickness. The corresponding skin friction results (see Ref.20 and below) are consistent with these trends: suction increases the skin friction level far upstream, whereas near the shock it is increased because of the suction - induced steepening of the adverse pressure gradient in this region.

3. Parametric Studies and Experimental Comparisons

3.1 Zero Mass Transfer

THEORETICAL RESULTS

A feature which is of great practical importance is the scaling effect (Reynolds number) on the interaction pressure field; the present prediction for this is shown in Fig. 8. It is seen that there is a significant Reynolds number effect even in the unseparated case: the extent of the interaction upstream and downstream of the incident shock decreases with increasing Reynolds number, tending toward a solution typical of the response to a simple step pressure rise at very high Reynolds number in agreement with the trends of the available experimental data [7,21,22]. Moreover, at the boundary layer edge the strengths of the local shock jump and post-shock expansion increase and decrease, respectively, with increasing Reynolds number; at sufficiently high Re_L the post-shock expansion region becomes very small and weak and hence difficult to detect experimentally.

Another important aspect of fundamental and practical interest is the characteristic upstream influence distance (here defined as the distance X_{up} upstream of the shock where the local interaction-induced pressure rise is only 5% of the overall total). The present theoretical predictions for this at various shock strengths as a function of Reynolds number are shown in Fig. 9, plotted as the ratio of X_{up} to the basic (non-interacted) boundary layer thickness δ_o (which also of course experience Mach and Reynolds effects). These values are of order unity($X_{up} \sim \delta_o$) as we should indeed expect for the "short-range" type of interactions characteristic of turbulent boundary layers [23]. It is seen from Fig. 9 that the upstream influence decreases markedly with both the shock strength and Reynolds number, in agreement with both experimental observations [7,21] and numerical simulations [24] in transonic flows. At moderate Reynolds numbers, X_{up}/δ_o decreases monotonically with Re_L approximately as a power law, whereas it tends to become independent of Reynolds number (perhaps even increasing slightly with Re_L) at very high Re_L. These conclusions agree with the predictions of

strong interaction theory for turbulent flows as recently shown by Inger[23].

Using the pressure solutions in the y-momentum equation and then integrating twice with respect to x along $y = \delta$ yields detailed expressions[5,8] for the interaction-induced interface displacement (boundary layer displacement thickness change) $\Delta Y/\delta_o$. This interaction growth of the boundary layer is often of practical interest, expecially in the interpretation of channel flow interaction experiments as discussed in detail elsewhere[25]. The influence of Reynolds number on this thickning is shown in Fig. 10. It is seen to decrease significantly with increasing Reynolds number, which is consistent with the aforementioned pressure distribution trends and again in qualitative agreement with experiment[7,21] and numerical simulations[24]. It is to be noted that the downstream asymptotic values are 5 to 8 times larger when expressed in terms of displacement thickness δ_o^* instead of δ_o, so that even the linearized theory prediction of the interaction effect on downstream boundary layer displacement thickness is generally quite significant (ranging from 25% to 50% under typical experimental conditions).

We now turn to the disturbance skin friction upstream of the shock. The results of a parametric study of this important property are presented in Fig. 11, which shows the Reynolds number effect on the local ratio $C_f(x)/C_{f_o}$ at various shock strengths and illustrates how C_f typically decreases toward the shock owing to the adverse pressure gradient disturbance induced by the shock-boundary layer interaction. It is also seen that increasing shock Mach number enhances this drop in skin friction owing to the stronger local interaction pressure gradient involved. In fact, when the interaction is strong enough, the present theory predicts vanishing skin friction below or ahead of the shock at lower Reynolds numbers. Although this result tends to overpredict the interaction effect on skin friction owing to the linearized small disturbance approximation in Eq. 8 (see, e.g., the discussion in Ref. 9) the theory is nevertheless useful for inferring basic qualitative trends. For example, it can be seen that Reynolds number

has the expected large influence on the skin friction and incipient separation behavior: the relative effect of the interaction at a given shock strength decreases significantly with Re_L while separation moves noticeably upstream with increasing shock strength and decreasing Reynolds number, all of which are in qualitative agreement with experimental trends[7,21] and the results of Navier-Stokes numerical calculations[24].

EXPERIMENTAL COMPARISONS

Although an appreciable body of data on transonic shock-boundary layer interactions has accumulated, most of these tests involve high Mach numbers ($M \gtrsim 1.3 - 1.4$) with a distinct lambda-shock interaction pattern and definite boundary layer separation and hence cannot be compared meaningfully with the present theory. However, there are a few unseparated experimental cases with which direct comparisons are possible.

Inclusion of the $\partial p/\partial y$ effect in the present theory enables a comparison of its predictions for the local interaction-pressure jump across the shock at the boundary layer edge versus shock strength against the various experimental values tabulated in Ref. 26 (Fig. 12). Within its realm of validity (unseparated flow, $M_1 < 1.3$) the theory is in good agreement with the data and shows the correct trend of approaching the full inviscid Rankine-Hugoniot value with increasing M_1 or Reynolds number.

A careful study of the available NAE wind tunnel tests of supercritical airfoil sections [27] identified two interaction cases suitable for comparison. The measured pressure distributions and correspondig theoretical predictions (based on the local pre-shock Mach number and Reynolds number conditions at the experimentally-observed shock location) are shown in Fig. 13. The theory is seen to predict the upstream influence well, whereas it overestimates the pressure recovery downstream. This is typical of such airfoil tests and is apparently caused by the fact that, in contrast to the normal incident shock theoretically assumed, the actual shock occurring in airfoil experiments is usually

oblique (albeit still with subsonic post-shock flow) owing to the non-uniform nature of the surrounding inviscid flow [14] (further discussion of this will be found in a forth-coming paper); the actual overall shock pressure rise in transonic flow can thus be 20 - 30 % lower than the normal shock value at the same incoming flow Mach number. Nevertheless, viewed overall the theory predicts the major features of the interaction fairly well. The final zero-mass transfer comparison that can be shown involves the wall pressure distributions at three Mach numbers from the classical interaction experiments of Ackeret, Feldman and Rott[7] (see Fig. 14). The general features of the interaction are seen to be correctly predicted; as expected, the linearized theory increasingly underestimates the upstream pressures with increasing shock strength. The overestimated downstream pressure recovery observed in these examples, which grows worse with increasing shock strength, is traceable to the channel flow blockage effect of the interaction - induced boundary layer thickening, which reduces the effective shock strength[14].

3.2 Mass Transfer Effects

THEORY

The influence of the basic mass transfer parameter B on the various physical properties of a typical interaction case is shown in Figs. 15A-D, from which a number of interesting conclusion can be drawn. Even moderate amounts of suction significantly reduce the overall streamwise extent of the interaction and steepen the adverse wall pressure gradient, whereas blowing has equally the opposite effect. Concordant with these trends, suction also strengthens the local shock jump at the boundary layer edge while reducing (perhaps even eliminating at high enough B) the degree and extent of the post-shock expansion region (Fig. 15B). The corresponding thickening effect of the interaction shown in Fig. 15C is very significantly influenced by mass transfer; for example, the moderate suction value $B = -.0003$ reduces $\Delta Y(\infty)$ nearly five-fold. The influence of B on the interactive skin

friction (Fig. 15D) is composed of two opposing effects: far upstream, the skin friction-increasing effect of suction dominates (which tends to delay separation) whereas closer to the shock the suction-induced steepening of the local adverse pressure gradient becomes important tending to reduce the local C_f. The former effect tends to dominate at small B where suction significantly inhibits separation; however, if B is sufficiently large it is possible in some weaker shock cases that the latter effect takes over and suction actually has a slightly adverse effect on separation (see Fig. 16).

It is noted that the influence of Reynolds number on the mass transfer effect was also studied[20]; suffice it here to state that it is similar to the zero mass transfer case for the values of B cited in Fig. 15.

The mass transfer effect on the upstream influence distance for various shock strengths and Reynolds numbers is shown in Fig. 17: suction reduces this influence more effectively for weaker shocks, the effect being linear in B for very small B. The corresponding downstream boundary layer thickening effect vs. B is presented in Fig. 18, showing the strong influence of mass transfer on the overall interaction.

EXPERIMENTAL EVIDENCE

To the authors knowledge, no quantitative interaction data are presently available pertaining to transonic shock-boundary layer interactions in the presence of wall mass transfer. However, some qualitative observations have been made in a channel flow [28] which lend support to the foregoing results: see Fig. 19. The Schlieren photos in the Figure show (a) the typical interaction pattern and (b) the qualitative effect of an unspecified amount of suction on it, including an evident thinning out of the boundary layer and reducing of the separation zone as implied by the present theory. The corresponding wall pressures measurements on the wall opposite the interaction (Fig. 19B), while only of qualitative value in analyzing the downstream interaction field, nevertheless clearly show evidence of the theoretically-predicted reduction of both upstream influence and downstream interactive-thickening* due to

*This reduced thickening results in a higher downstream interaction pressure owing to the smaller channel flow blockage [14].

suction. Such reductions were also observed to be significant in experiments on a supersonic compressive interaction flow[29]; furthermore, delay of the separation in the upstream free interaction region was obtained, again in qualitative agreement with the suction effect predicted by the present theory.

4. Concluding Remarks

It is felt that the present work establishes the value of the theoretical model involved as a tool for engineering studies of non-separting transonic normal shock - turbulent boundary layer interactions including the important influence of wall suction or blowing. Nevertheless, it is worthwhile in conclusion to reemphasize certain limitations which warrant improvement in future theoretical studies.

The primary limitation in the theory is of course the linearized disturbance approximation that restricts it to only weak incident shocks. The primary consequences of this approximation are two-fold: one, the distortion of the incoming boundary layer profile and thickness is not fed back into the local disturbance solution as it proceeds along the interaction, resulting in an underestimate of the interaction pressures near the shock (e.g. Fig. 14) that increases with shock strength; two, the nonlinear viscous effects on the flow in the frictional sublayer are neglected, leading to an overestimate of the skin friction disturbance and a premature incipient separation prediction that becomes very large with increasing shock strength. As regards the former, a recent investigation by Panaras and Inger[12] has suggested an approximate means of treating the nonlinear profile-distortion effects in terms of the overall shape factor change; further work is in progress to incorporate suction and blowing effects. Concerning the latter, an improved nonlinear "lower deck" theory is required, for example along the lines of an approximate boundary layer-type integral method such as used by Tu and Weinbaum[30]. Study of such an improvement is underway by the senior author to provide a more accurate interactive skin friction throughout the complete M_1 - Re_L range of non-separated interactive conditions. With such an improved nonlinear feature, the important question of incipient separation and its control by suction can then be accurately, fundamentally addressed without need for the present-day empiricisms.

Acknowledgements

The present work was supported by the U.S. Office of Naval Research under Contract N 00014 - 75 -C - 0456. The assistance of the Von Humboldt Foundation to the senior author is also gratefully acknowledged.

References

1. Pearcey, H.H., "Shock-Induced Separation and It's Prevention by Design and Boundary Layer Control", in Boundary Layer and Flow Control (G. Lachman, Ed.), Pergamon, 1961

2. Peake, D.J., H. Yoshihara, D. Zonars and W. Carter, " The Transonic Performance of Two-Dimensional Jet-Flapped Airfoils at High Reynolds Numbers", in AGARD CP-83 Facilities and Techniques for Testing at Transonic Speeds, pp. 7-1 to 7-39, April 1971.

3. Bore, C.L., " On the Possibility of Deducing High Reynolds Number Characteristics Using Boundary Layer Suction", Ibid, pp. 23-1 to 23-9.

4. Green, J.E., "Some Aspects of Viscous - Inviscid Interactions at Transonic Speeds and Their Dependence on Reynolds Number", Ibid, pp. 2-1 to 2-12.

5. Inger, G.R. and W.H. Mason, "Analytical Theory of Transonic Normal Shock-Boundary Layer Interaction", AIAA Journal, 14, pp. 1266-72, Sept. 1976.

6. Liepman, H.W., " The Interaction Between Boundary Layer and Shock Waves in Transonic Flow", Journal of the Aeronautical Sci., 13, Dec. 1946, pp. 623-637.

7. Ackeret, J., F. Feldman, and N. Rott, "Investigations of Compression Shocks and Boundary Layers in Gases Moving at High Speed," NACA TM-1113, Jan. 1947.

8. Mason, W.H. and G. R. Inger, "Analytical Study of Transonic Normal Shock-Boundary Layer Interaction," VPI & SU Report Aero-027, Blacksburg, Va., Nov. 1974.

9. Lighthill, M.J., "On Boundary Layers and Upstream Influence; II, Supersonic Flow Without Separation," Proc. Royal Soc., A 217, No. 1131, pp. 478-507, 1953.

10. Inger, G.R., "Compressible Boundary Layer Flow Past a Swept Wavy Wall with Heat Transfer and Ablation," Astronautica Acta 19, pp. 325-338, 1971.

11. Inger, G.R., and E.P. Williams, "Subsonic and Supersonic Boundary-Layer Flow Past a Wavy Wall," AIAA J., Vol. 10, pp. 636-642, May 1972.

12. Panaras, A.G., and G.R. Inger, "Normal Shock - Boundary Layer Interaction in Transonic Speed in the Presence of Streamwise Pressure Gradient," ASME Paper 77-GT-34, International Gas Turbine Conf., Phil., Pa., April 1977.

13. Gadd, G.E., "Interactions between Normal Shock Waves and Turbulent Boundary Layers," British ARC Ref. 22559 (N.P.L. R & M 3262), Feb. 1961.

14. Melnik, R.E., and B. Grossman, "Analysis of the Interaction of a Weak Normal Shock Wave with a Turbulent Boundary Layer," AIAA Paper No. 74-598, June 17, 1974.

15. Chen, T.S., E.M. Sparrow and F.K. Tsou, "The Effect of Mainflow Transverse Velocities in Linear Stability Theory", Jour. Fluid Mech. 50, 4, 1971, pp. 741-50.

16. Dorrance, W.H., Viscous Hypersonic Flow, McGraw-Hill, 1962, pp. 218-219.

17. Kutateladze, S.S., and A.I. Leont'av, Turbulent Boundary Layers in Compressible Gases, Edward Arnold, London, 1964, p. 24.

18. Conrad, P., C. du P. Donaldson, and R. Snedeker, "A Study of the Model Response Approach to Patterned Ablation Including Experiment Definition," SAMSO TR-70-213, Aeronautical Research of Princeton, Inc., Princeton, New Jersey, 1969.

19. Martellucci, A., H. Rie, and J.R. Sontowski, "Evaluation of Several Eddy Viscosity Models Through Comparison with Measurements in Hypersonic Flows," AIAA Paper No. 69-688, June 1969.

20. Zee, S., "Parametric Study of a Theory for Transonic Normal Shock - Turbulent Boundary Layer Interaction," M.S. Thesis, Dept. of Aerospace and Ocean Eng., VPI & SU, Blacksburg, Va., Aug. 1976.

21. Vidal, R.J., C.E. Whitliff, P.A. Catlin, and B.H. Sheen, "Reynolds Number Effects on the Shock Wave-Turbulent Boundary Layer Interaction at Transonic Speeds," AIAA Paper 73-661, Palm Springs, Calif., July 1973.

22. Mateer, G.G., A. Brosli, and J.R. Viegas, "A Normal Shock Wave-Turbulent Boundary Layer Interaction at Transonic Speeds," AIAA Paper 76-161, Wash., D.C., Jan. 1976.

23. Inger, G.R., "Similitude Properties of High Speed Laminar and Turbulent Boundary Layer Incipient Separation", AIAA 9th Fluid and Plasma Dynamics Conf. Paper 76-375, San Diego (July 1976). To appear in AIAA Journal, May '77.

24. Deiwert, G.S., "Numerical Simulation of High Reynolds Number Transonic Flows", AIAA J. 13, pp. 1354-1359, Oct. 1975.

25. Inger, G.R., "Analysis of Transonic Normal Shock-Boundary Layer Interaction and Comparisons with Experiment", AIAA Paper 76-331, July 1976; VPI & SU Report Aero-053, Blacksburg, Va., Aug. 1976.

26. Lomax, M., F.R. Bailey, and W.F. Ballhaus, "On the Numerical Simulation Three-Dimensional Transonic Flow with Application to the C-141 Wing," NASA TN D-6933, Aug. 1973.

27. Ohman, L.M., J.J. Kacprzynski and D. Broun, "Some Results from Tests in the NAE High Reynolds Number Two-Dimensional Test Facility on 'Shockless' and other Airfoils," 8th ICAS Paper 72-33, Amsterdam, Sept. 1972.

28. LeBlanc, R., and R. Göthals, "Etude de Phenomenes d' Interaction Onde de Choc Normale - Couche Limit Turbulente," Centre d' Etudes Aerodynamiques et Thermiques, Univ. of Poitiers, Poitiers, France, Oct. 1974.

29. Gai, S.L., "Shock-Wave Boundary Layer Interaction with Suction," Zeit. für Flug. Wissenschaften und Weltraumforschung Band I, Heft2, März - April 1977.

30. Tu, K.M., and S. Weinbaum, "A Nonasymptotic Triple Deck Model for Supersonic Boundary Layer Interaction", AIAA Jour. 14, June 1976, pp. 767 - 775.

Figures

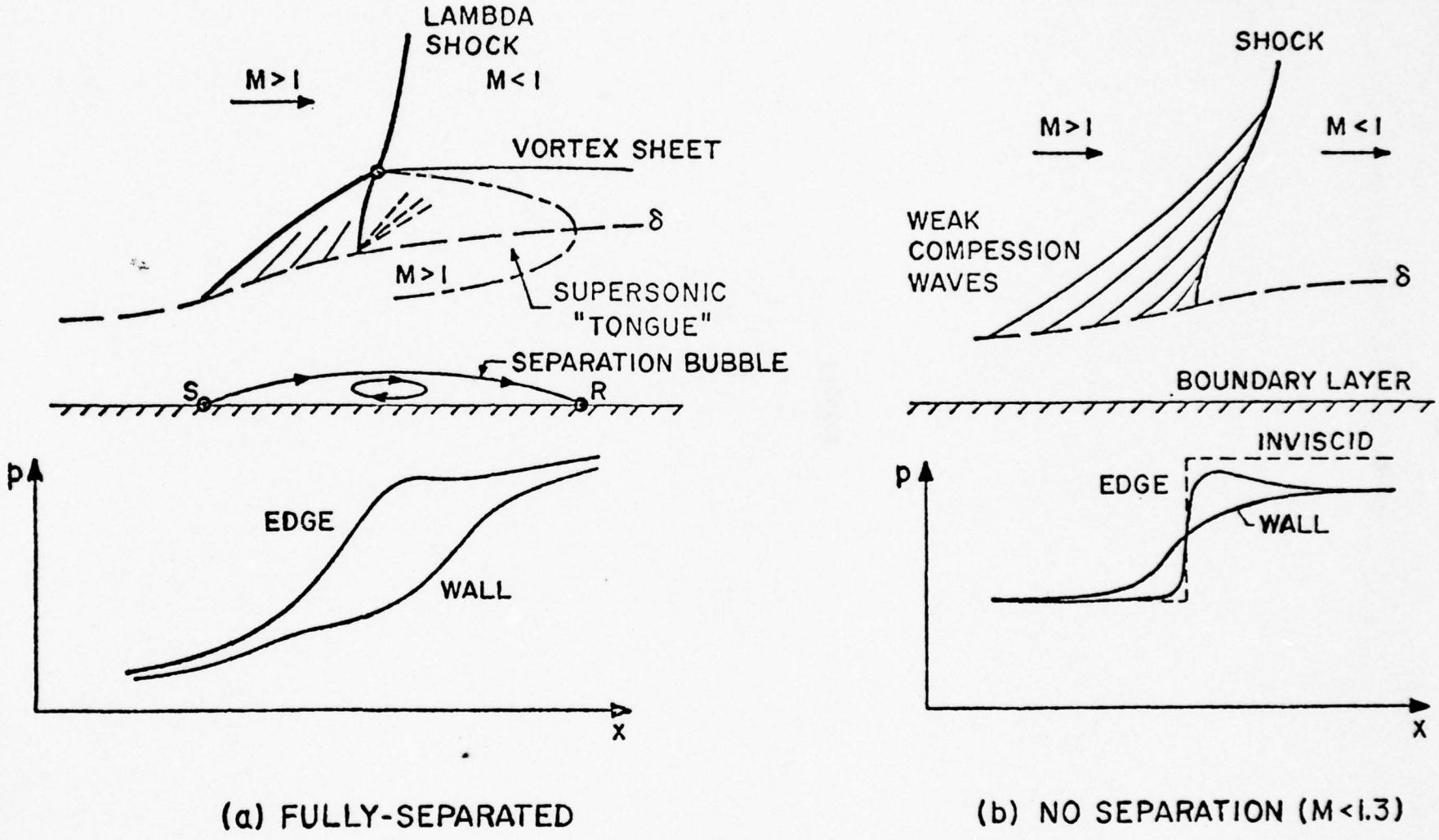

Fig. 1 Transonic Shock Turbulent Boundary Layer Interaction Flow Patterns

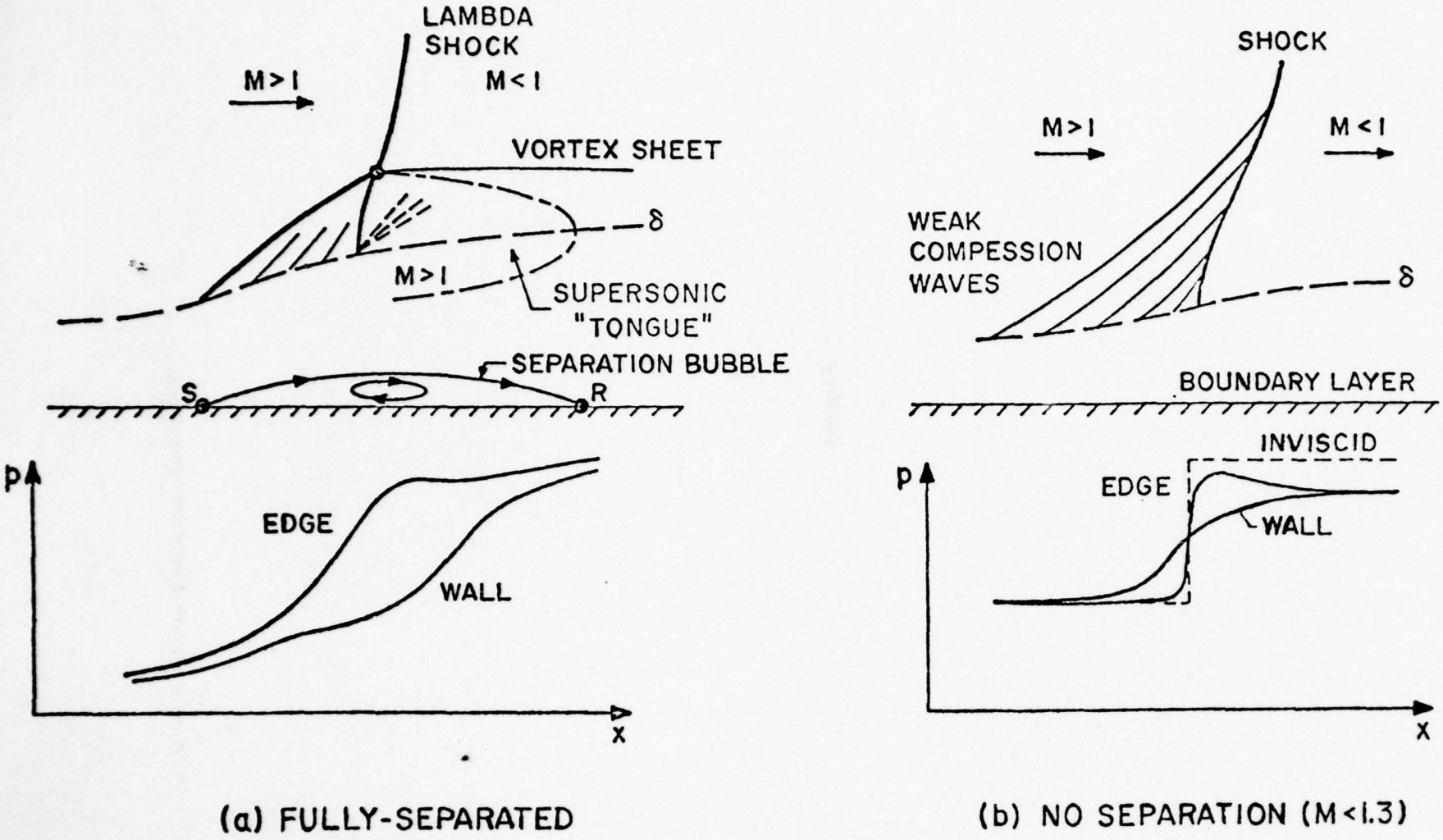

Fig. 1 Transonic Shock Turbulent Boundary Layer Interaction Flow Patterns

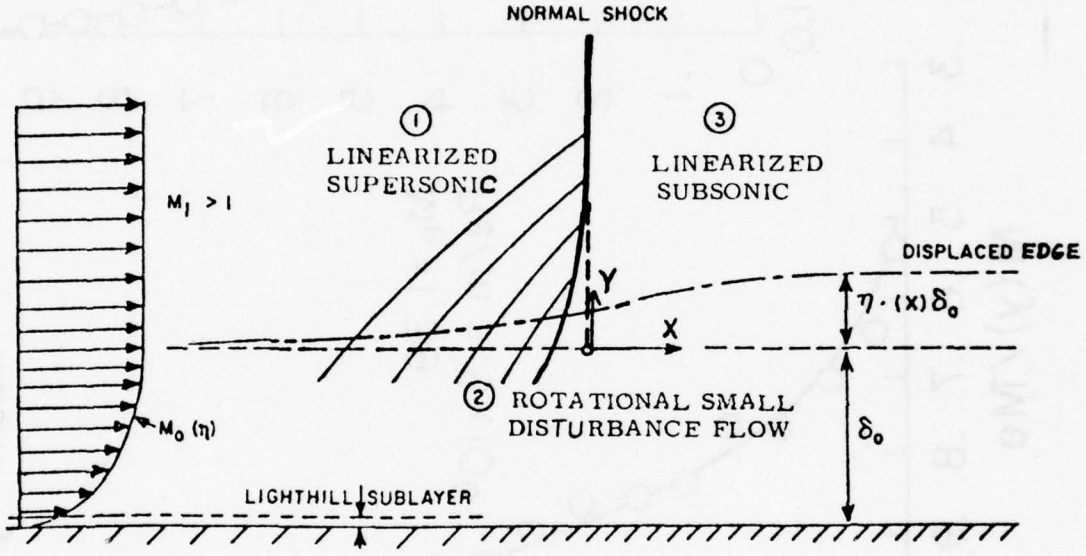

Fig. 2

Approximate Flow Model of Non-Separating Interactions

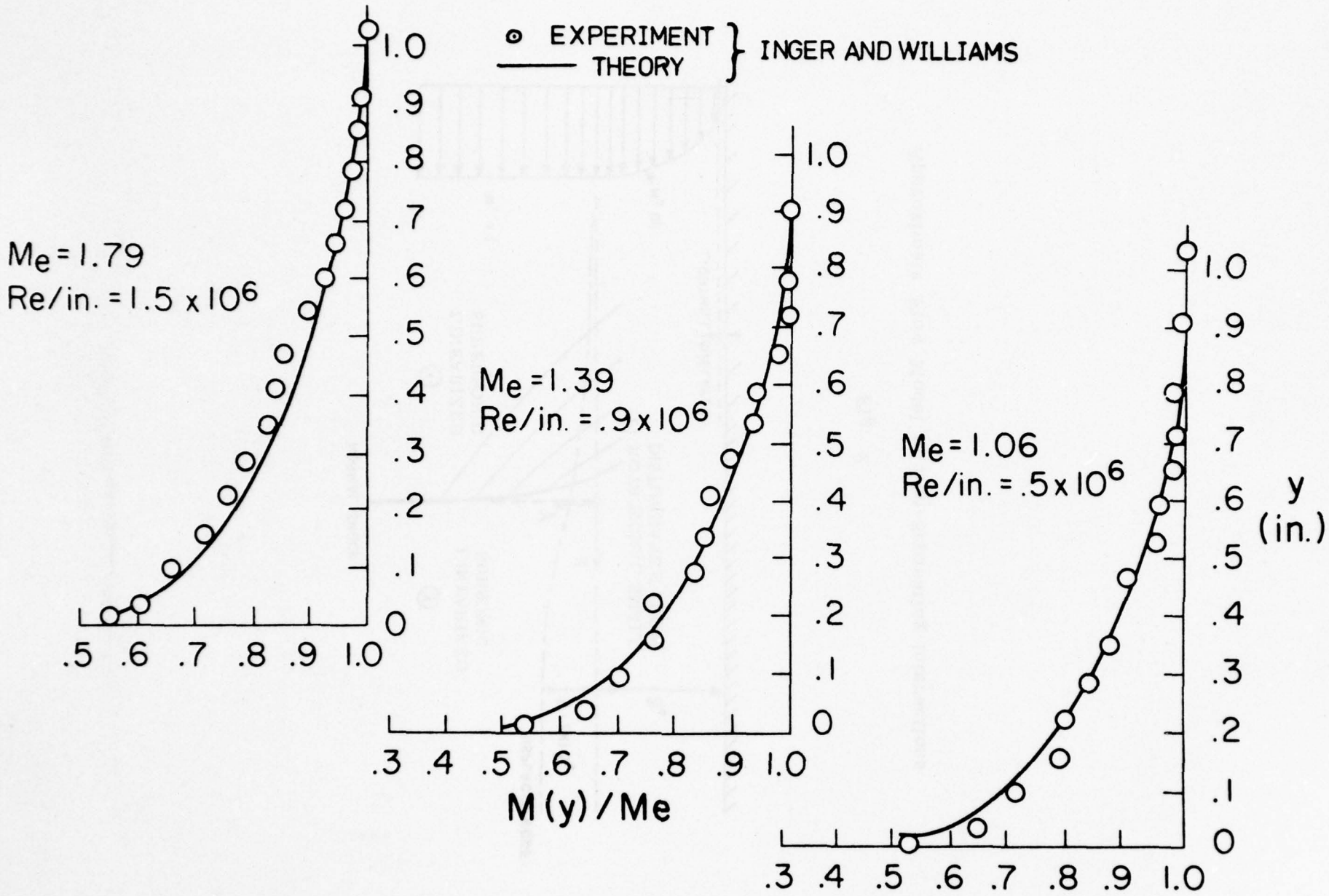

Fig. 3 Input Turbulent Boundary Layer Profile Model of Undisturbed Flow: Comparison with Experiment

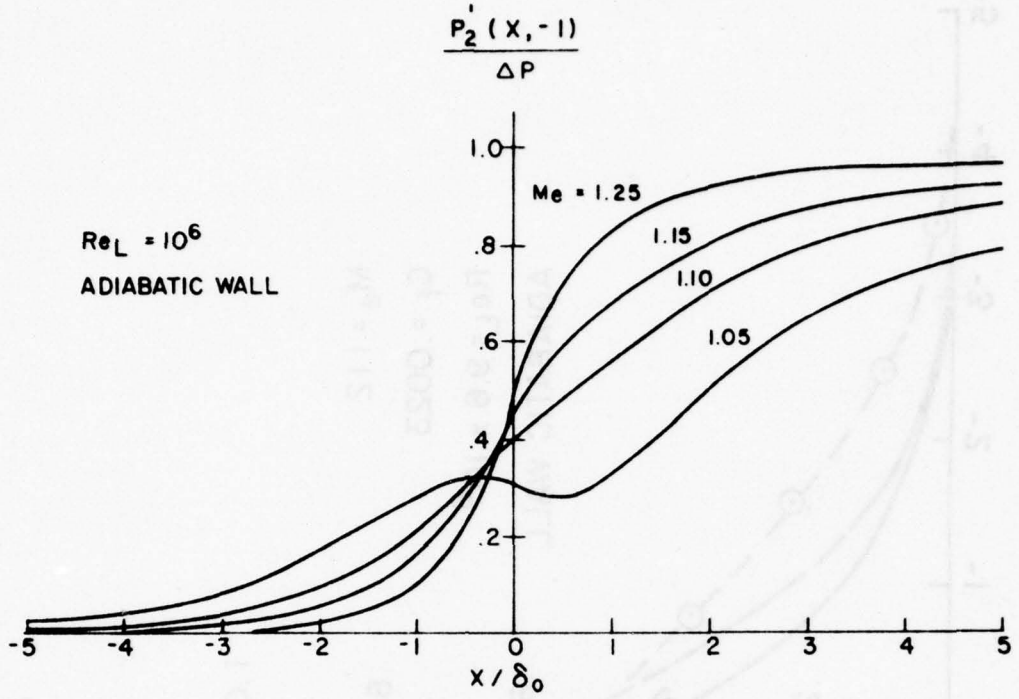

A. WALL PRESSURE

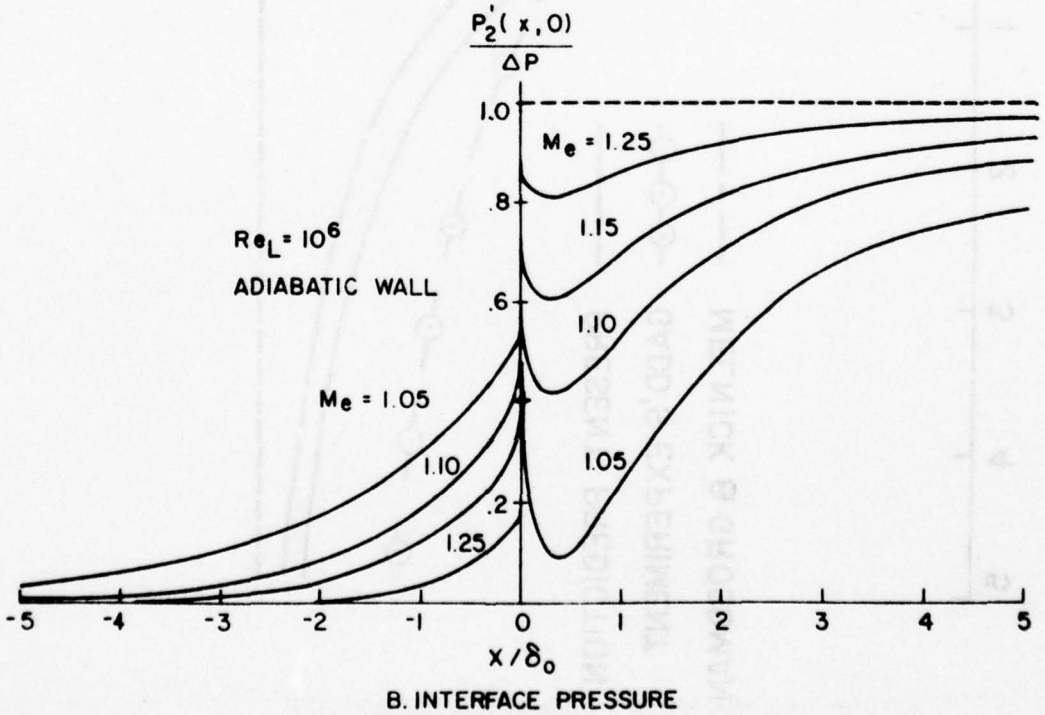

B. INTERFACE PRESSURE

Fig. 4 Typical Results for Interactive Pressure Field

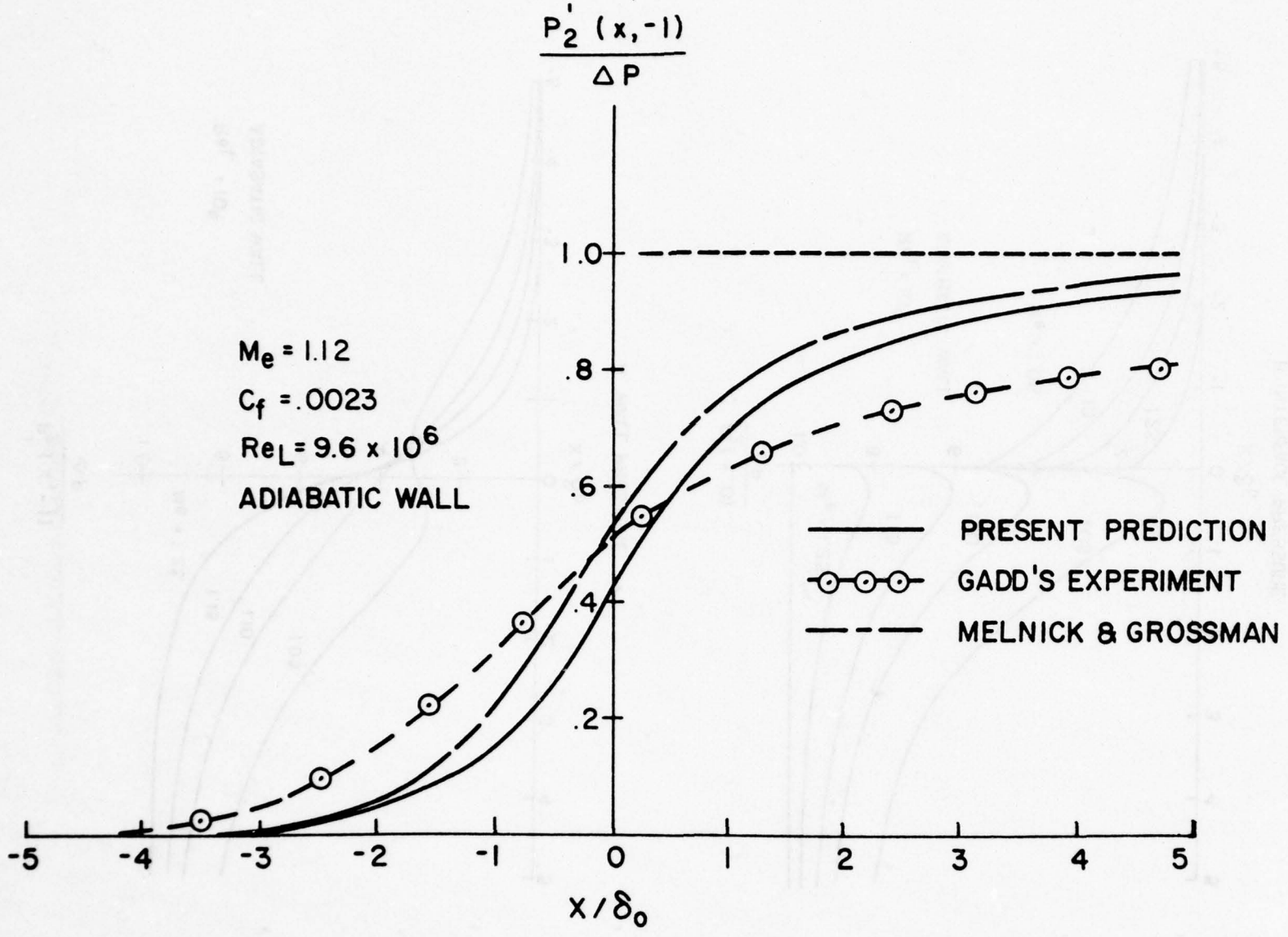

Fig. 5 Typical Theoretical Experimental Comparison for Pipe Flow

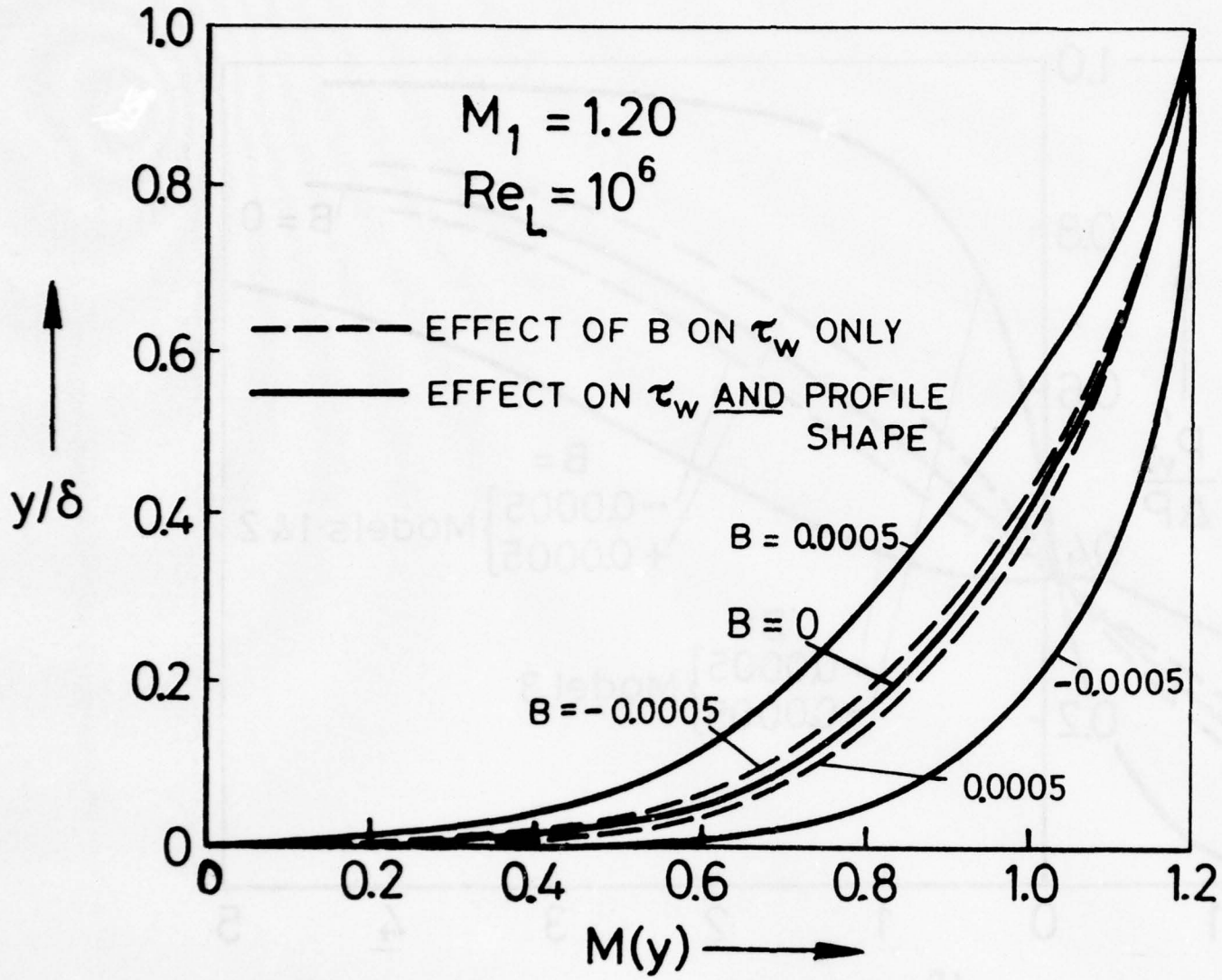

Fig. 6 Typical Mass Transfer Effect on Incoming Boundary Layer Mach Number Profile

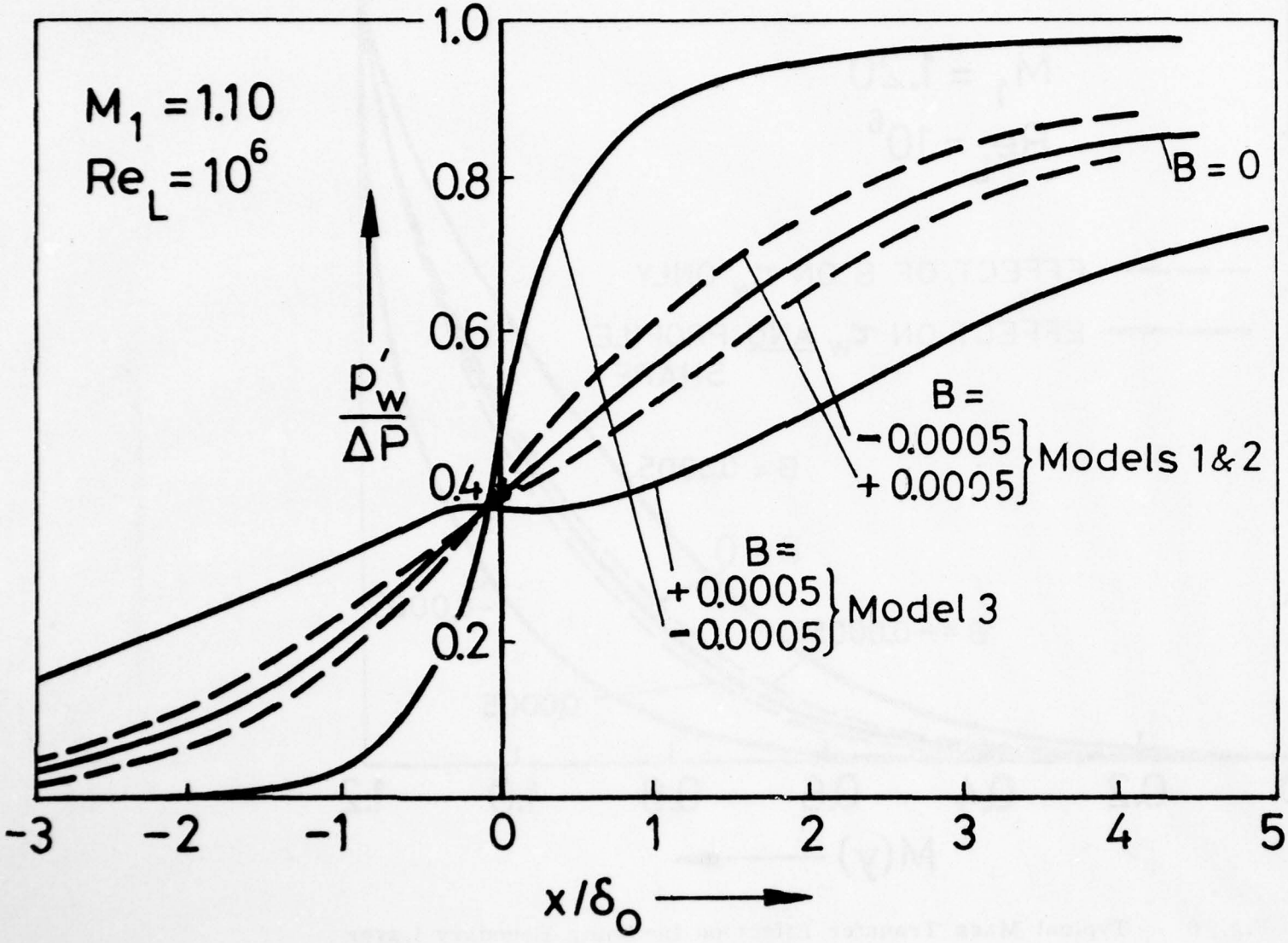

Fig. 7 Typical Blowing/Suction Influence on Interactive Wall Pressure Distribution

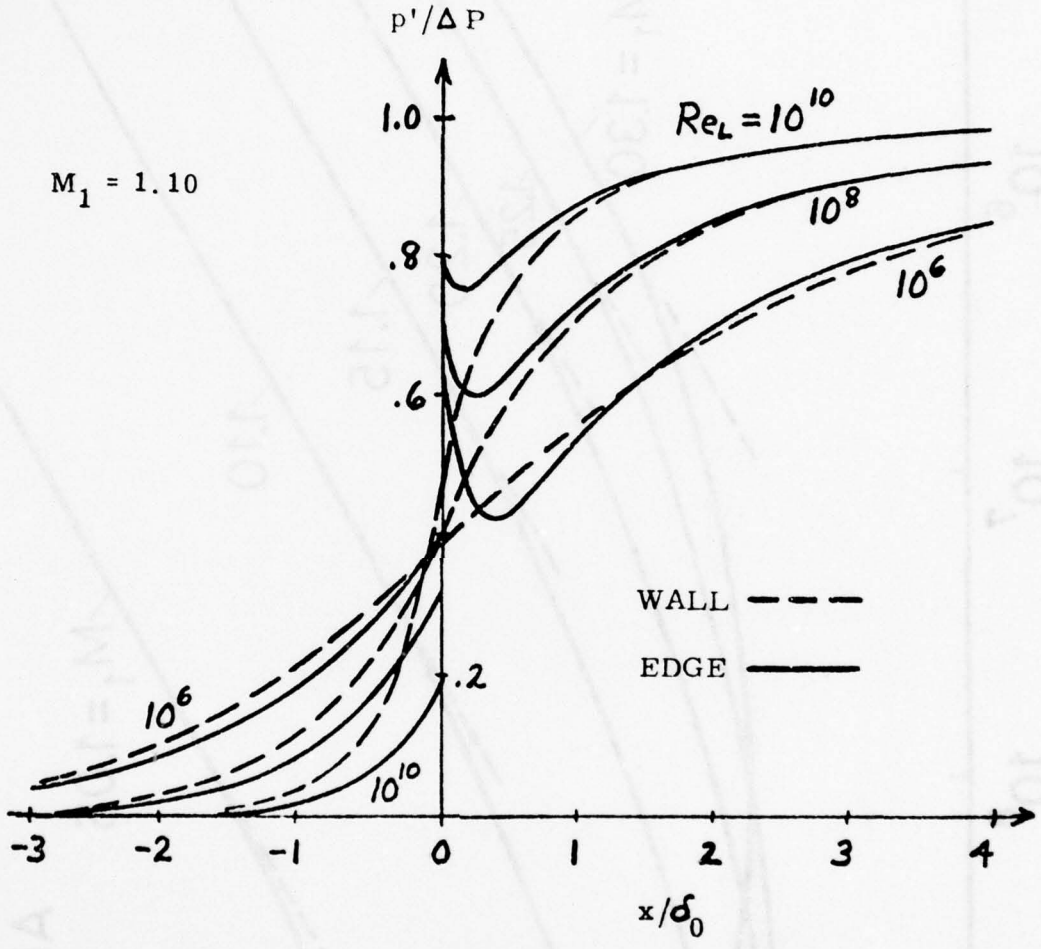

Fig. 8 Reynolds Number Effect on Interactive Pressures for a Typical Solid Wall Case

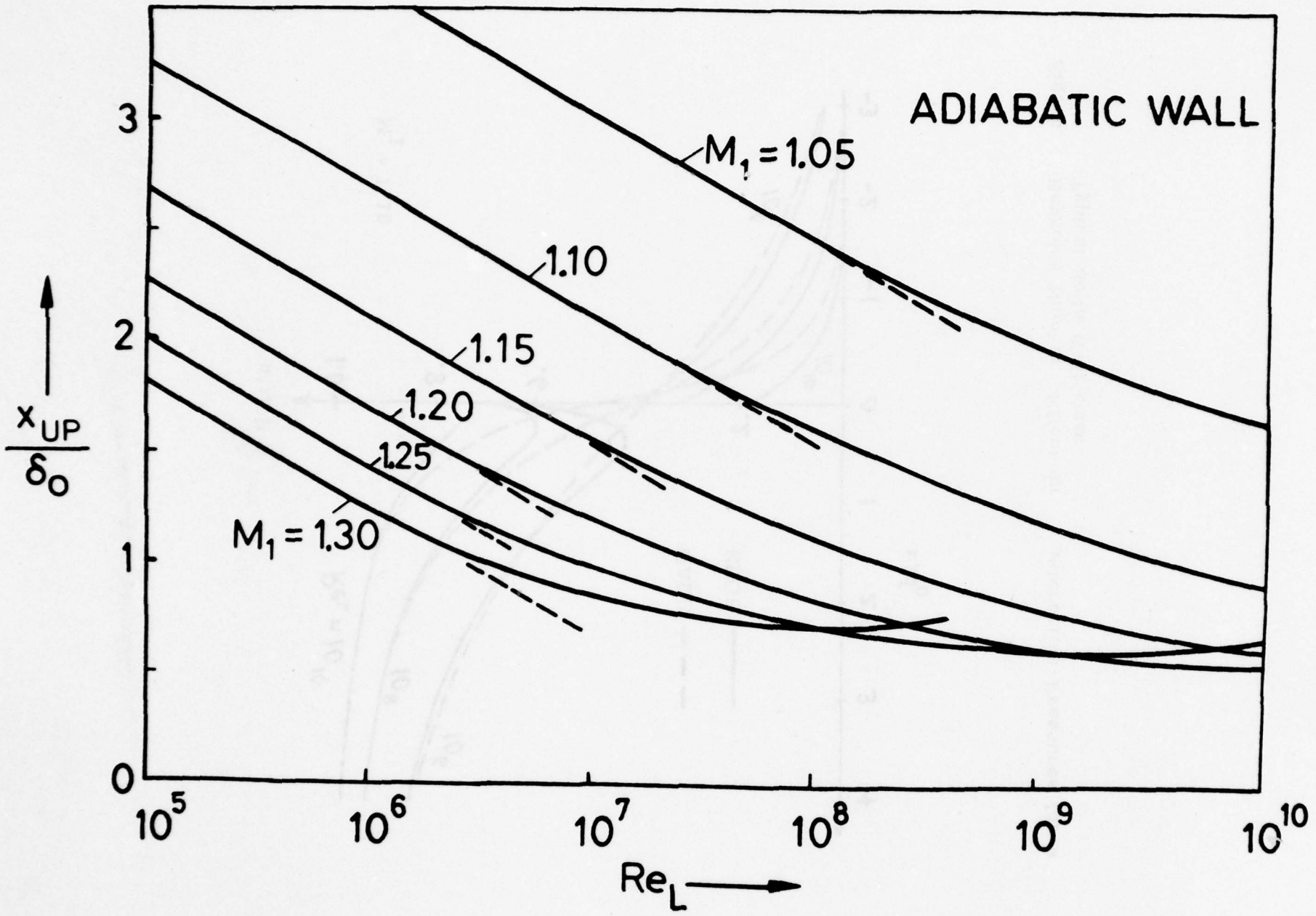

Fig. 9 Predicted Reynolds Number Effect on the Upstream Influence Distance vs. Incident Shock Strength

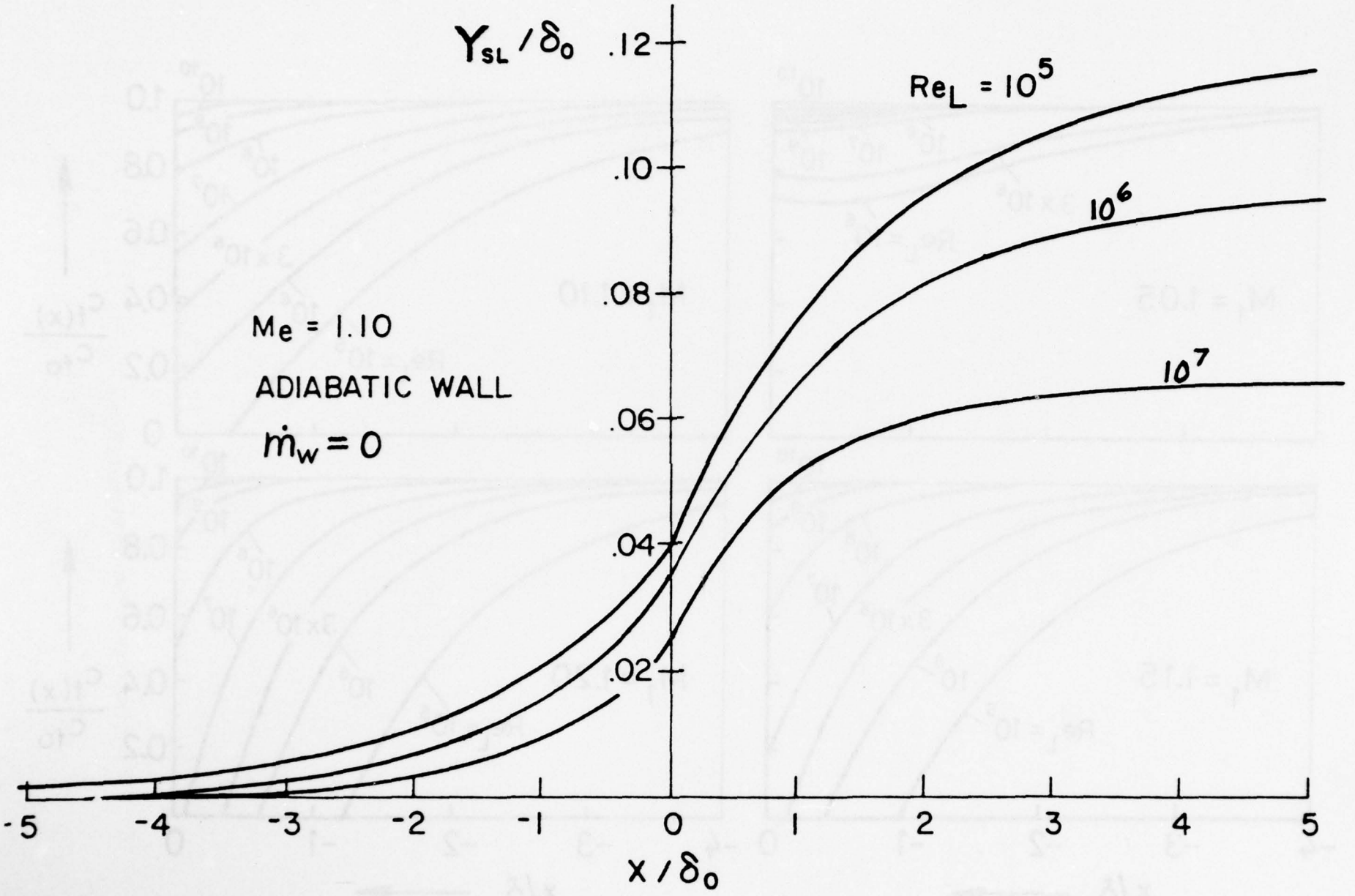

Fig. 10 Interaction - Induced Thickening of the Boundary Layer ($\dot{m}_w = 0$)

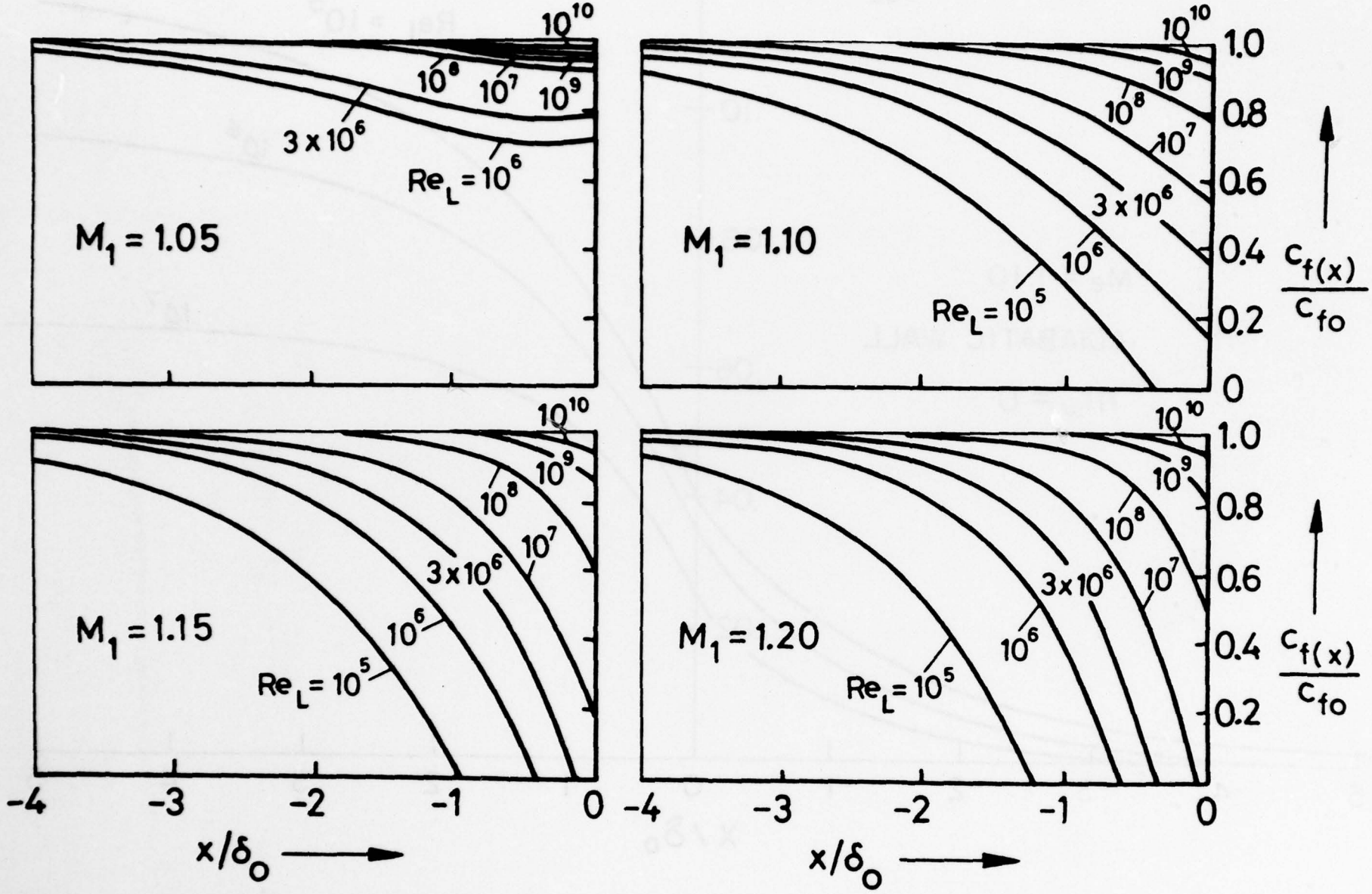

Fig. 11 Shock - Strength and Reynolds Number Effects on the Theoretical Local Interactive Skin Friction

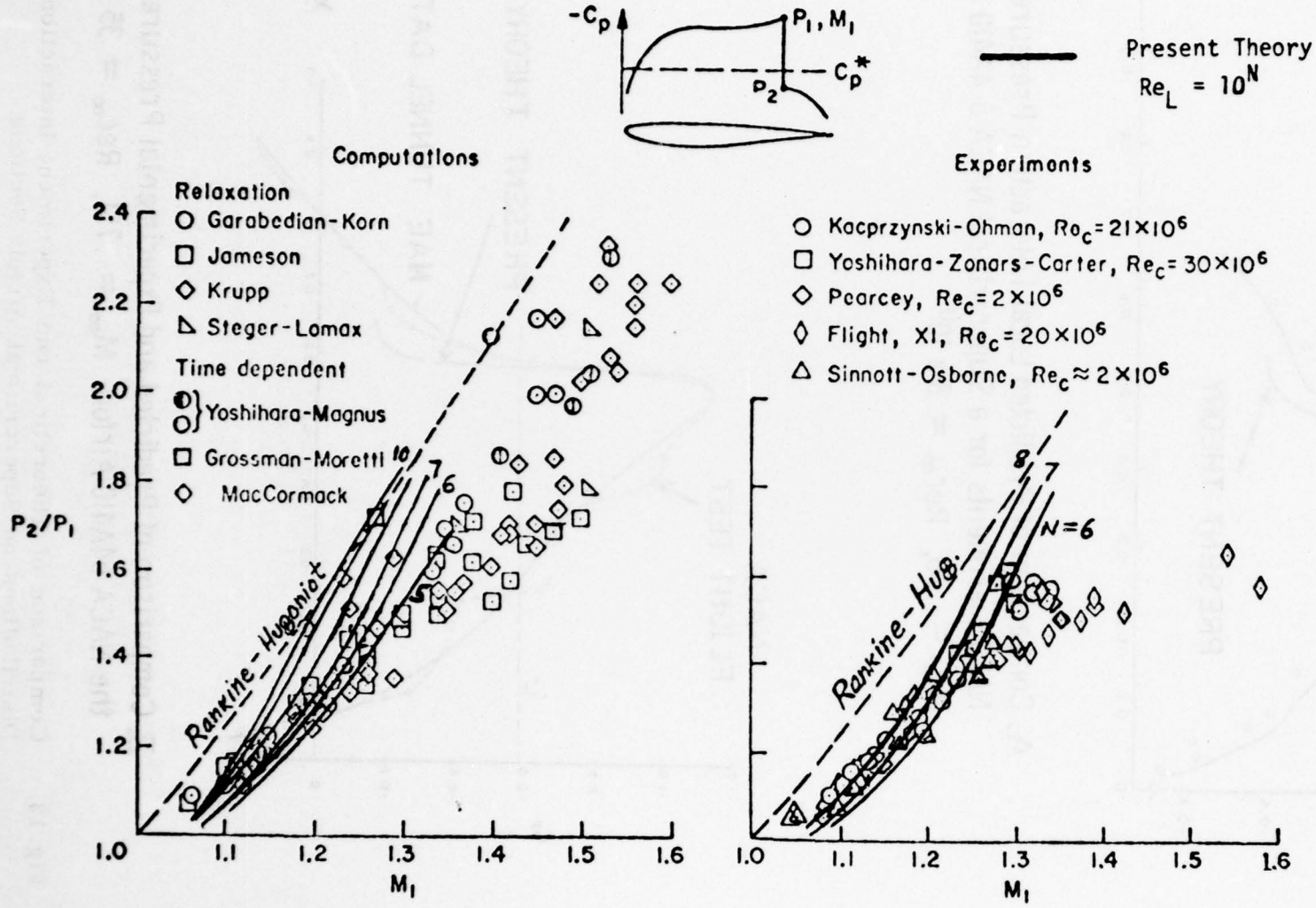

Fig. 12 Comparison of Theory and Experiment for Local Pressure Jump Across Shock at the Boundary Layer Edge

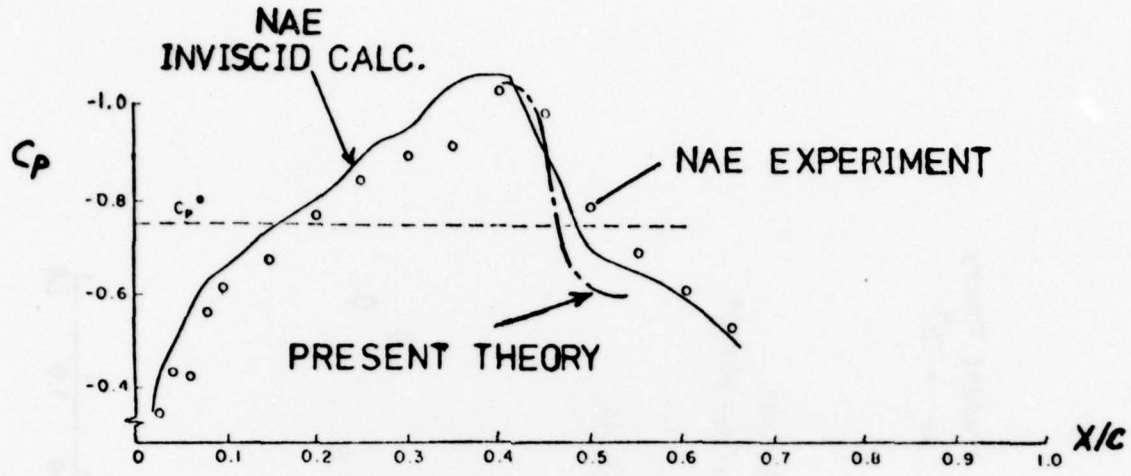

A. Comparison of Predicted Local Interaction Pressures with NAE Experiments for a Supercritical NACA 6 4A410 Airfoil: $M_\infty = .70$, $Rec_\infty = 8 \times 10^6$

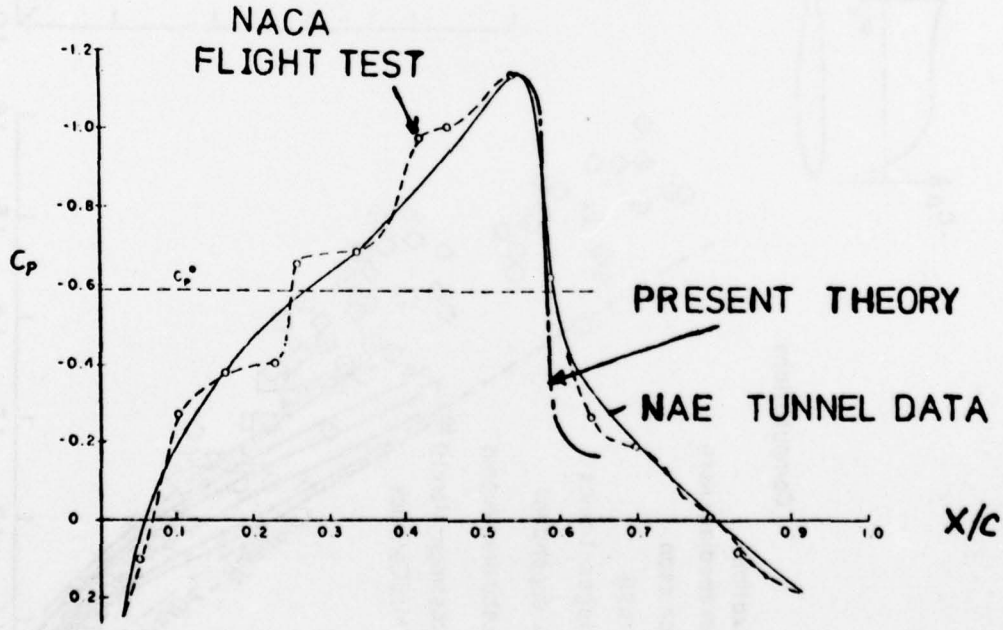

B. Comparison of Predicted and Experimental Pressures for the NACA 64A410 Airfoil: $M_\infty = .751$, $Rec_\infty = 35 \times 10^6$

Fig. 13 Comparison of Theoretical and Experiment Interaction Pressure Distributions on Supercritical Airfoil Sections

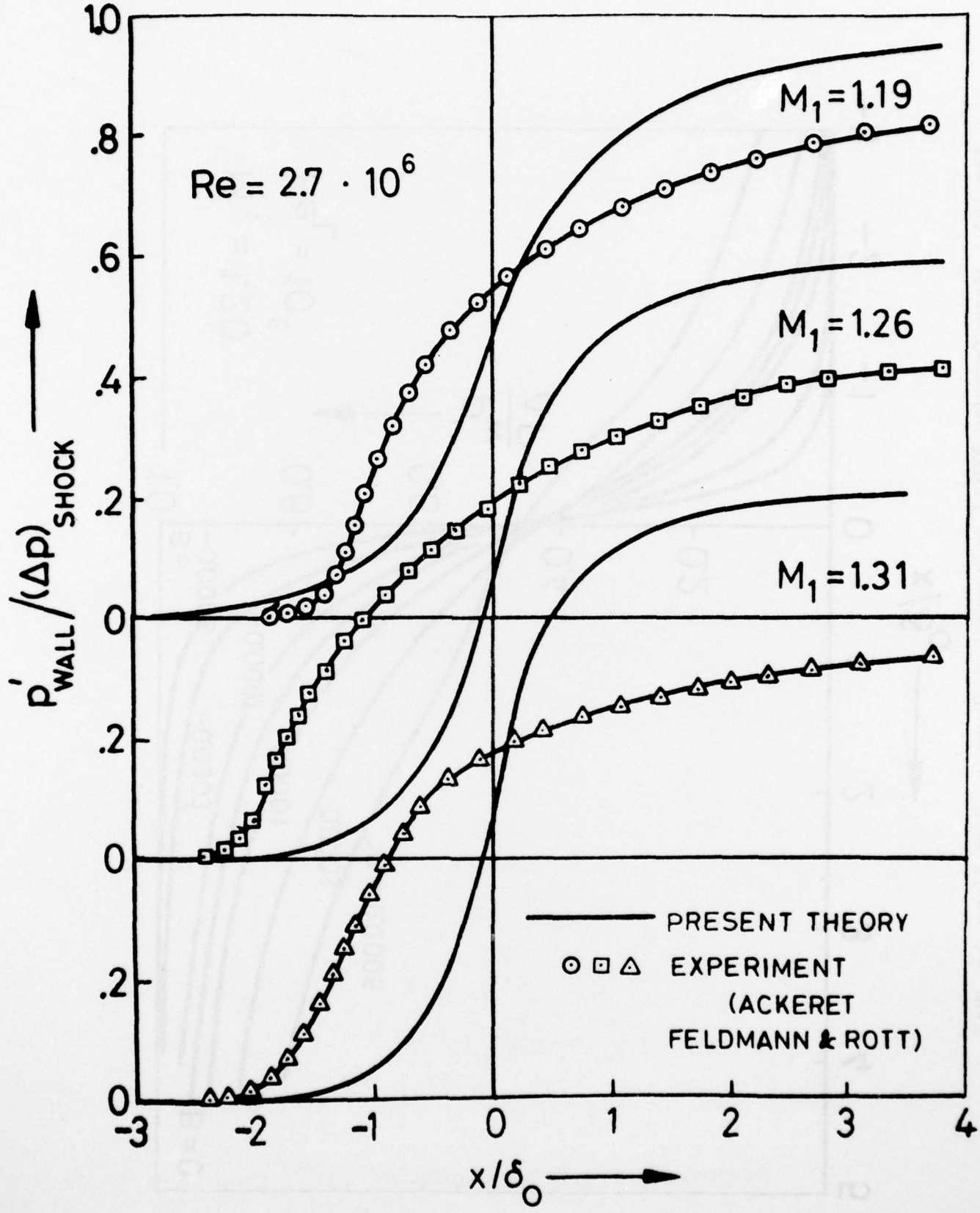

Fig. 14 Comparison of Pressures with the Channel Flow Measurements of Ackeret, Feldman and Rott[7]

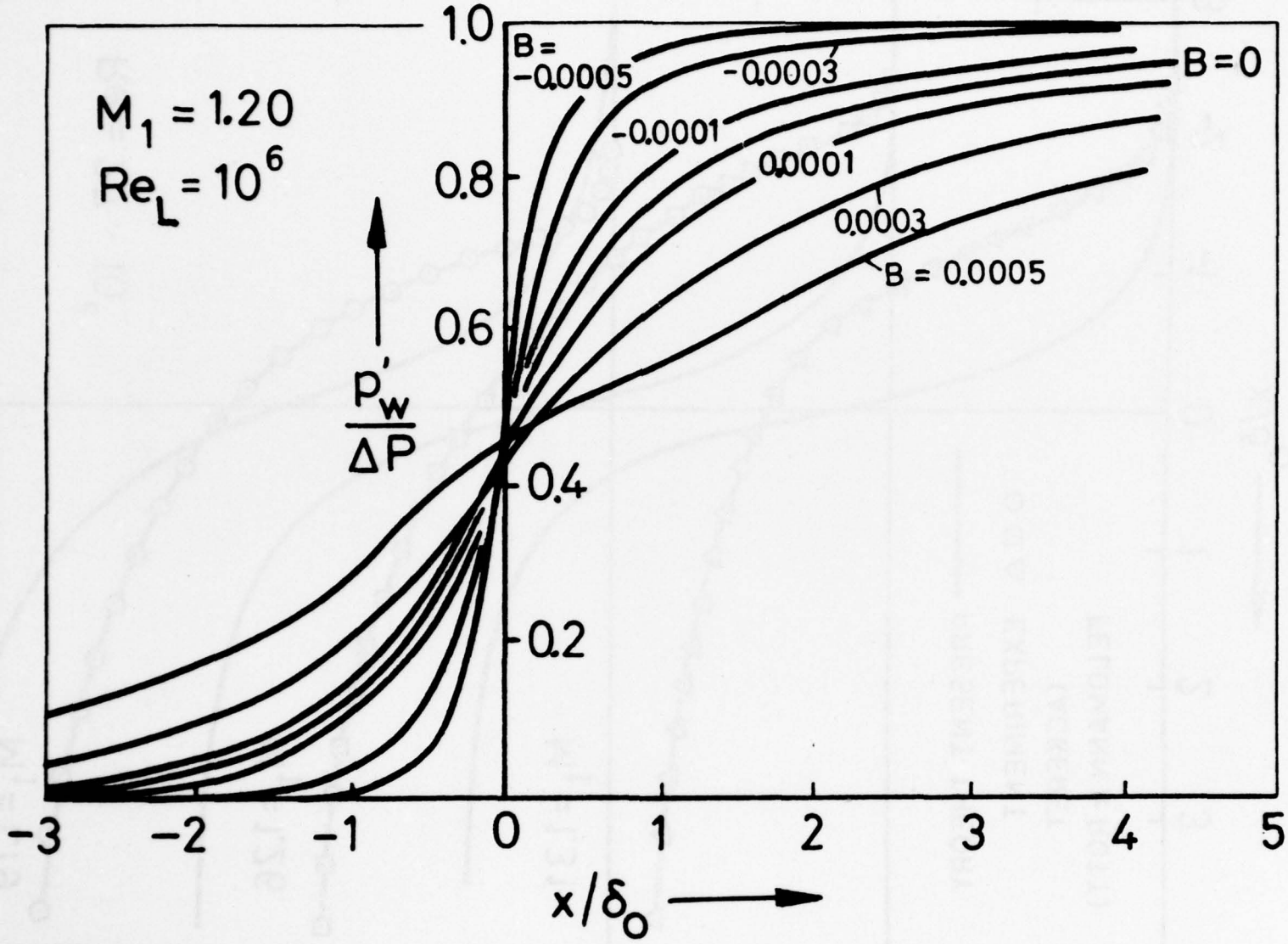

Fig. 15A Mass Transfer Effect on Interactive Pressure Rise Along the Wall

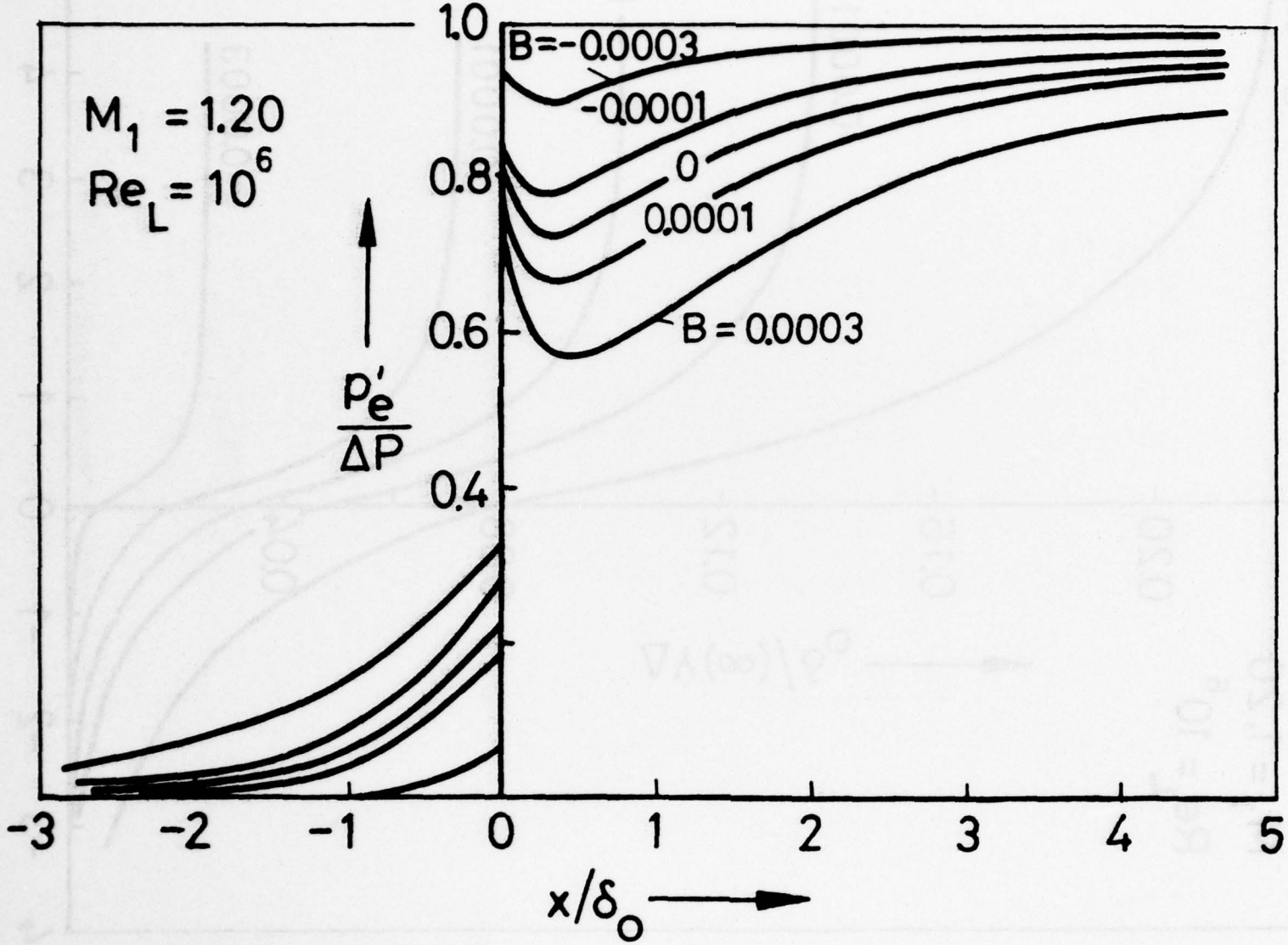

Fig. 15B Mass Transfer Effect on Interaction Pressure Along Edge of the Boundary Layer

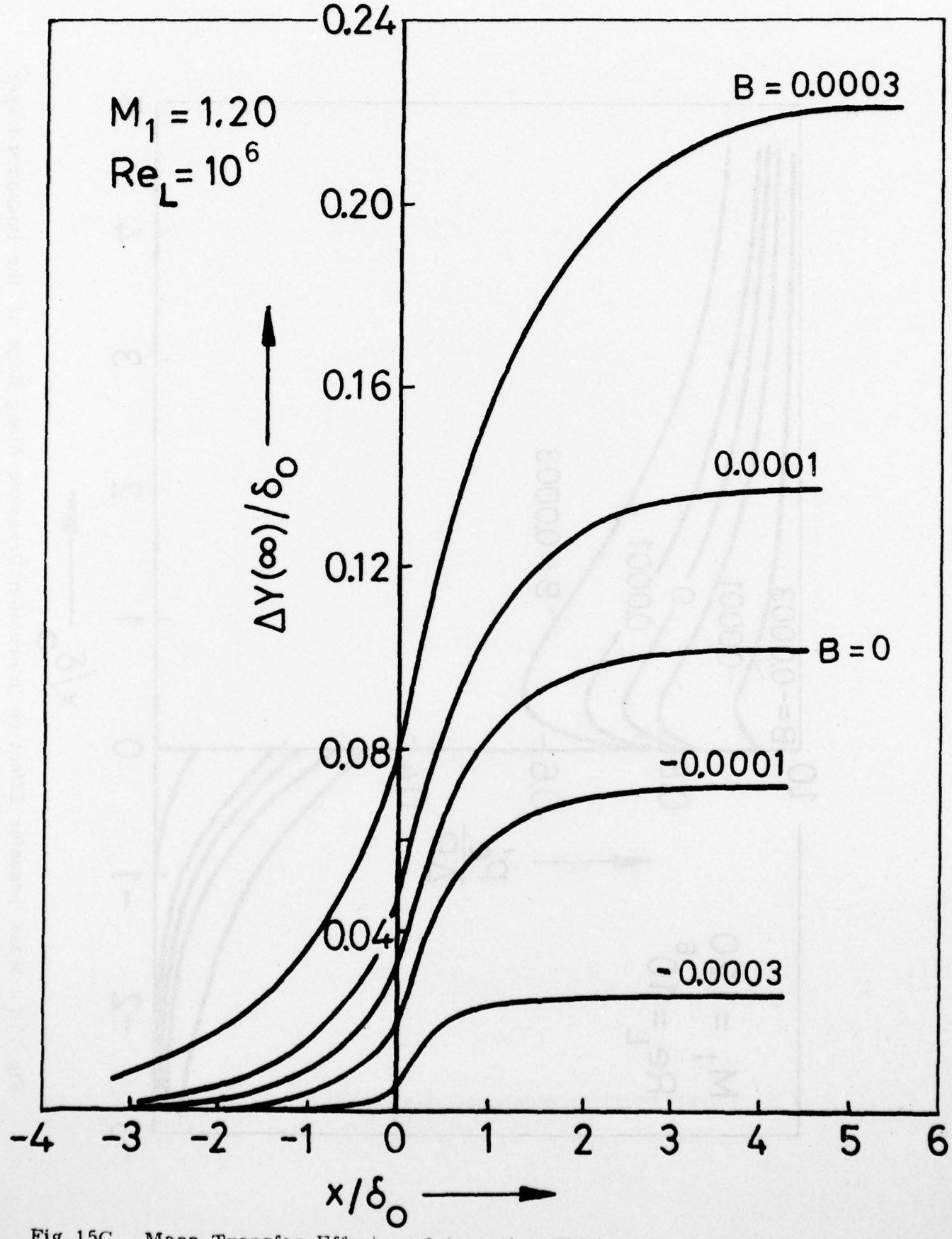

Fig. 15C Mass Transfer Effect on Interactive Thickening of the Boundary Layer

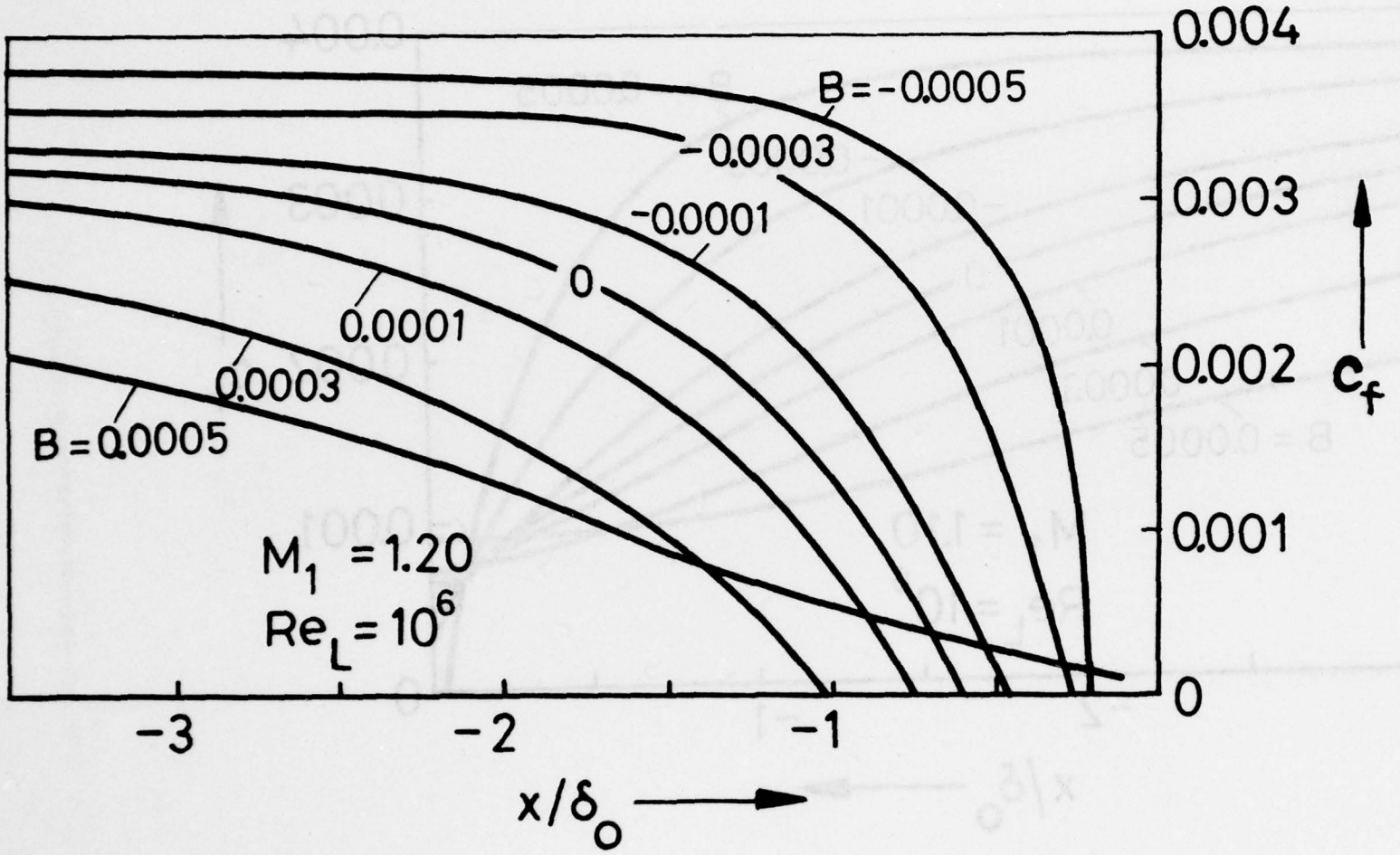

Fig. 15D Mass Transfer Effect on the Interactive Skin Friction Distribution

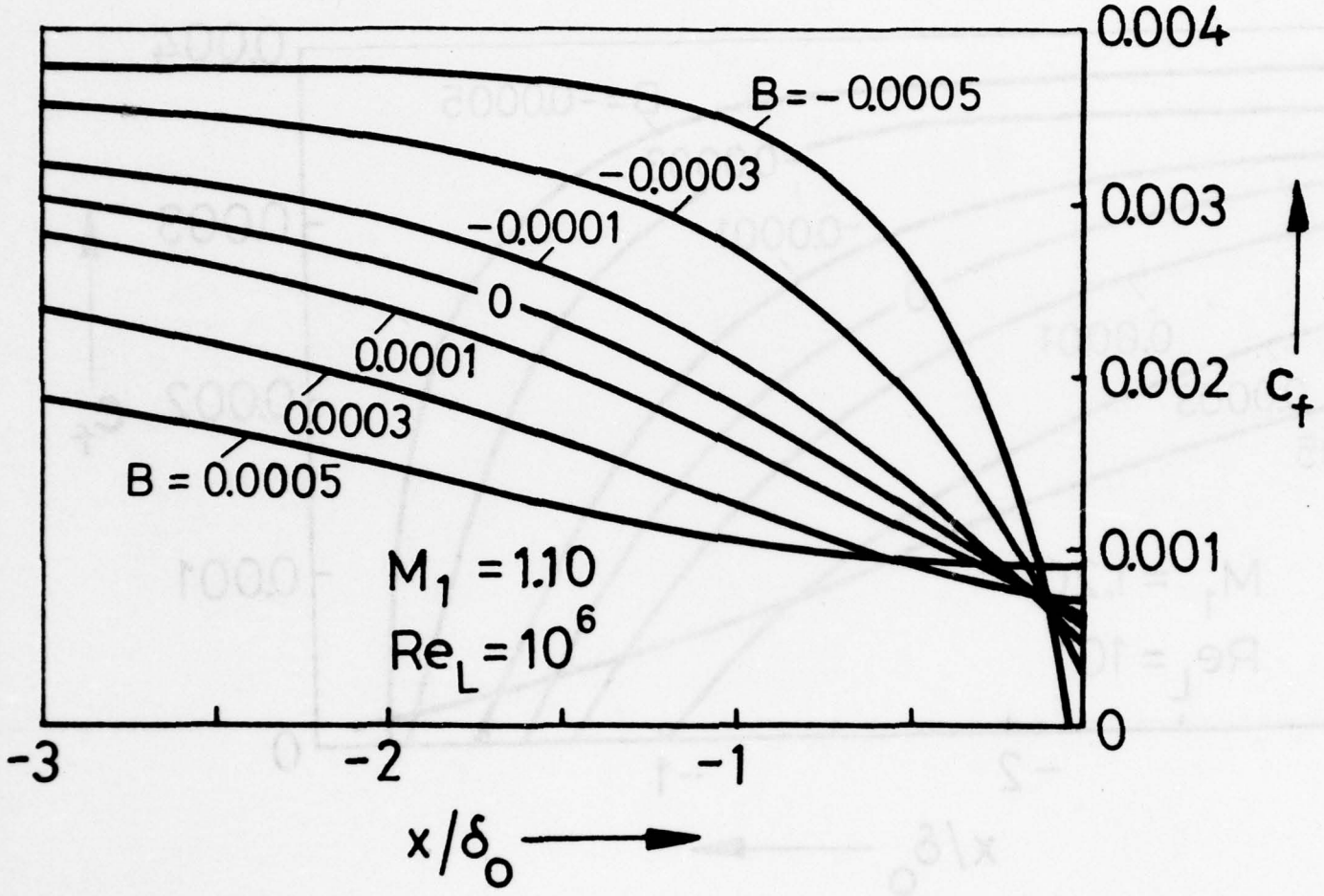

Fig. 16 Mass Transfer Effect on Interactive Skin Friction for Very Weak Shocks

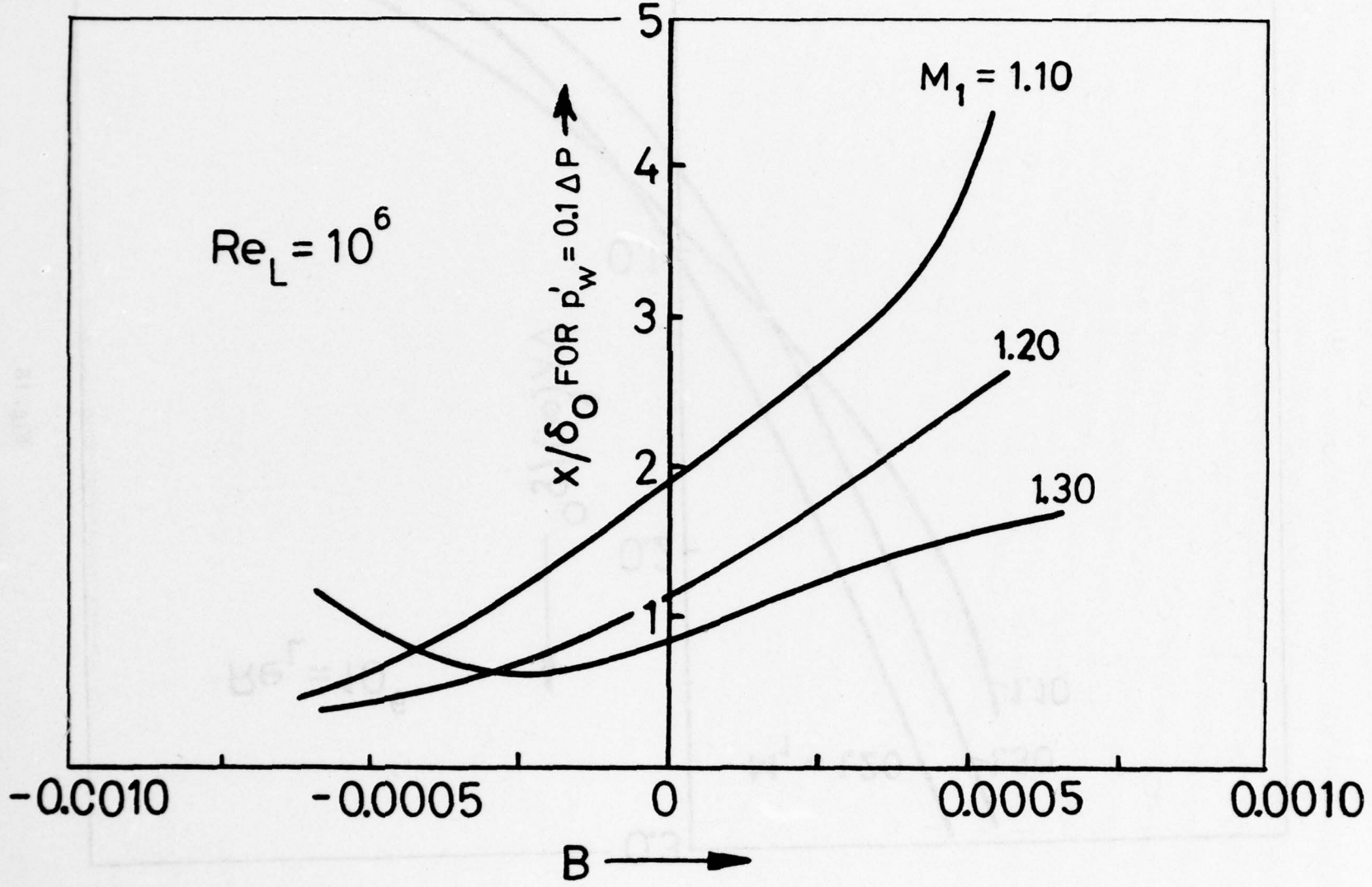

Fig. 17 Effect of Mass Transfer on Upstream Influence

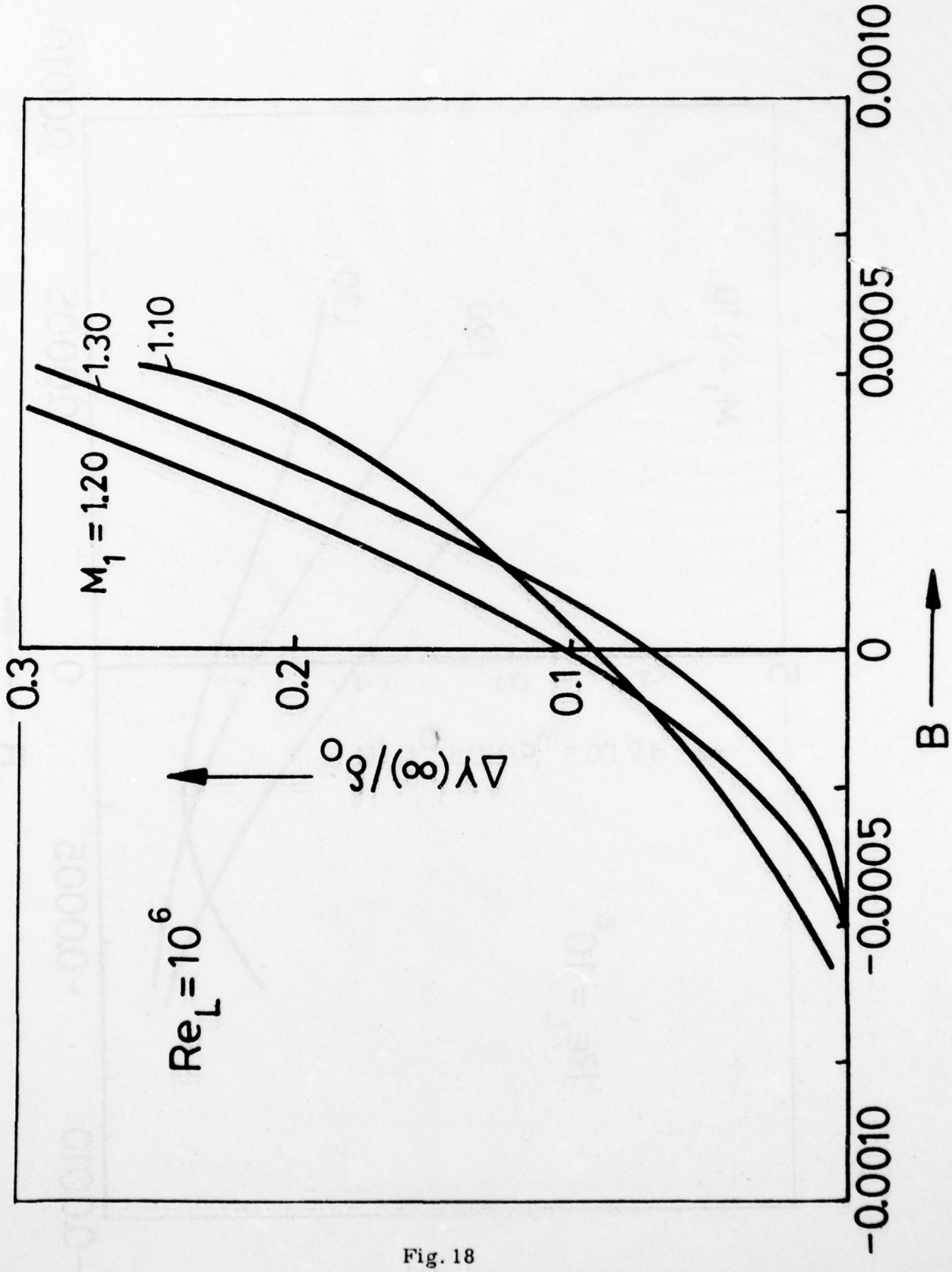

Fig. 18

Influence of Mass Transfer on Overall Interactive Thickening

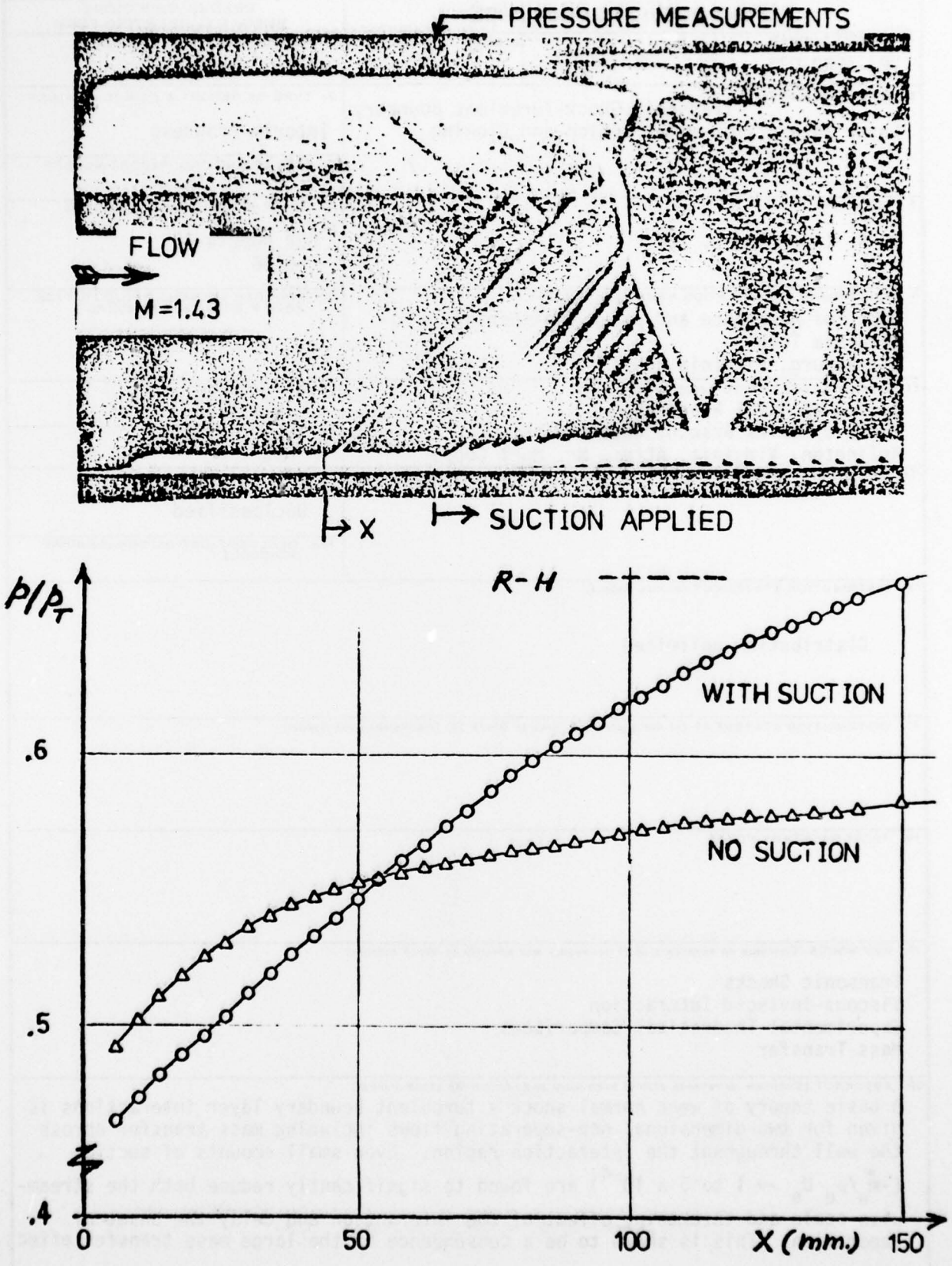

Fig. 19 Qualitative Experimental Confirmation of Theoretical Model Predictions: Suction Tests of Le Blanc

SECURITY CLASSIFICATION OF THIS PAGE *(When Data Entered)*

REPORT DOCUMENTATION PAGE

READ INSTRUCTIONS BEFORE COMPLETING FORM

1. REPORT NUMBER: VPI-AERO-073	2. GOVT ACCESSION NO.
3. RECIPIENT'S CATALOG NUMBER	
4. TITLE *(and Subtitle)*: Transonic Shock-Turbulent Boundary Layer Interaction with Suction and Blowing	5. TYPE OF REPORT & PERIOD COVERED: Interim Progress
	6. PERFORMING ORG. REPORT NUMBER
7. AUTHOR(s): G. R. Inger and S. Zee	8. CONTRACT OR GRANT NUMBER(s): ONR N00014-75 C-0456
9. PERFORMING ORGANIZATION NAME AND ADDRESS: Dept. of Aerospace and Ocean Engineering, Virginia Tech, Blacksburg, Virginia 24061	10. PROGRAM ELEMENT, PROJECT, TASK AREA & WORK UNIT NUMBERS
11. CONTROLLING OFFICE NAME AND ADDRESS: Office of Naval Research, Fluid Dynamics Branch, Code 438, Arlington, Virginia Attn: Mr. Mort Cooper	12. REPORT DATE: July 1977
	13. NUMBER OF PAGES: 53
14. MONITORING AGENCY NAME & ADDRESS *(if different from Controlling Office)*	15. SECURITY CLASS. *(of this report)*: Unclassified
	15a. DECLASSIFICATION/DOWNGRADING SCHEDULE

16. DISTRIBUTION STATEMENT *(of this Report)*

Distribution unlimited

17. DISTRIBUTION STATEMENT *(of the abstract entered in Block 20, if different from Report)*

18. SUPPLEMENTARY NOTES

19. KEY WORDS *(Continue on reverse side if necessary and identify by block number)*

Transonic Shocks
Viscous-Inviscid Interaction
Experimental-Theoretical Comparisons
Mass Transfer

20. ABSTRACT *(Continue on reverse side if necessary and identify by block number)*

A basic theory of weak normal shock - turbulent boundary layer interactions is given for two-dimensional non-separating flows including mass transfer across the wall throughout the interaction region. Even small amounts of suction ($-\dot{m}_w/\rho_e U_e \sim 1$ to 5×10^{-4}) are found to significantly reduce both the streamwise scale and thickening effect of the interaction and delay the onset of separation. This is shown to be a consequence of the large mass transfer effect

DD FORM 1 JAN 73 1473 EDITION OF 1 NOV 65 IS OBSOLETE

SECURITY CLASSIFICATION OF THIS PAGE *(When Data Entered)*

on the shape of the incoming boundary layer Mach number profile away from the wall. Parametric study results showing the influence of Reynolds and shock Mach number as well as mass transfer parameter on the interaction, plus favorable comparisons with various experimental data, are also presented.